Archaeometric and Archaeological Characterization of the Fired Clay Brick Production in the Brussels-Capital Region between the XIV and the Third Quarter of the XVIII Centuries (Belgium)

Caractérisation archéométrique et archéologique de la production briquetière de la Région de Bruxelles-Capitale entre le XIV^e siècle et le troisième quart du XVIII^e siècle (Belgique)

Eric Goemaere[a], Philippe Sosnowska[b], Mark Golitko[c], Thomas Goovaerts[a] and Thierry Leduc[a]

Abstract: Brick samples from different archaeological sites represent mostly houses in Brussels (Belgium) built between the end of the Middle ages (end of 13th-beginning 14th centuries) and the end of the Modern Period (18th century). The study gives a mineralogical–petrographical–chemical characterization of the brick samples made in the Brussels-Region and sources the raw silty material, the moulding sand and the lime-mortar. Optical microscopy, X-ray powder diffractometry, Laser Ablation Inductively Coupled Plasma Mass Spectrometry, magnetic susceptibility and scanning electron microscopic with an energy dispersive X-ray attachment were applied both to fired clay bricks and regional clayey materials. Bricks were moulded with a silica rich, non-calcareous loam gathered locally in the alluvial plain of the Senne valley. Material from gleysols and fluvisols were mined separately to shape two types of bricks. A strong chemical resemblance with the thick loessic deposits of the Belgian plateaus results from erosion and river transport and sedimentation in the wide alluvial plain of Brussels. Petrography and geochemistry show minor participation of marine Lower Palaeozoic, Cretaceous and Tertiary rocks from the alimentation area of the Senne. Although clayey tertiary layers outcrop in the Brussels Region and are cut by the numerous tributaries of the Senne valley, they were never exploited for brick making in the Brussels Capital Region. Mineralogical composition and petrography suggest the absence of mixing with river sand or local marine tertiary sands. Local sediments extracted in the valley sides as Eocene fossiliferous fine sand were used as moulding sand.

Résumé : *Les briques étudiées proviennent majoritairement d'habitations construites à Bruxelles (Belgique) entre la fin du Moyen Âge (fin XIII^e-début XIV^e siècle) et la fin des temps Modernes (XVIII^e siècle). L'étude fournit une caractérisation minéralogique, pétrographique et chimique des briques faites dans la Région de Bruxelles Capitale et discute des sources des matières premières silteuses, les sables de moulage et les mortiers de chaux. La microscopie optique, la diffraction des rayons X, l'ablation laser associée à la spectrométrie de masse à couplage inductif, la susceptibilité magnétique et la microscopie électronique à balayage couplée aux analyses par analyse dispersive en énergie, furent utilisées pour caractériser les briques et différentes ressources argileuses régionales. Les briques ont été moulées avec une matière première silteuse, riche en silice, non calcareuse et récoltée localement dans la plaine alluviale de la vallée de la Senne. Des gleys et des fluvisols ont été extraits séparément pour la préparation de deux types de briques. La forte ressemblance chimique*

[a] *Geological Survey of Belgium, Earth & History of Life O.D., Royal Belgian Institute of Natural Sciences, 13 Rue Jenner, 1000, Brussels, Belgium. (egoemaere@naturalsciences.be) (tleduc@naturalsciences.be), (tgoovaerts@naturalsciences.be)*

[b] *Université libre de Bruxelles (ULB), Research Centre for Archaeology and Heritage (RCAH) and research group Construction Histories Brussel (CHsB), Brussels, Belgium. (philippe.sosnowska@ulb.ac.be)*

[c] *University of Notre Dame, Department of Anthropology, 621, Flanner Hall, Notre Dame, Indiana, 46556, USA. (mgolitko@nd.edu) & The Field Museum of Natural History, Integrative Research Center, Social Science, 1400 S. Lake Shore Drive, Chicago, Illinois 60605, USA.*

rec. fév. 2007 ; acc. nov. 2007

avec les épais dépôts lœssiques de plateaux résulte de l'érosion de ces derniers et de leur transport par la rivière suivi de la sédimentation dans la large plaine alluviale de Bruxelles. La pétrographie et la géochimie montrent une participation mineure de roches sédimentaires du Paléozoïque inférieur, du Crétacé et du Tertiaire issues du bassin d'alimentation de la Senne. Bien que les couches de sédiments meubles argileux du Tertiaire affleurant en Région Bruxelloise soient recoupées par les nombreux affluents de la Senne, elles n'ont jamais été utilisées pour la production de briques dans la Région de Bruxelles Capitale. La composition minéralogique et la pétrographie suggèrent l'absence d'ajout de sables de rivières ou de sables marins tertiaires locaux. Des sables fossilifères fins d'âge Eocène sont utilisés comme sable de moulage.

Keywords: bricks, Middle Ages, archaeometric analyses, alluvial deposits, sourcing, Brussels.

Mots clés : *briques, Moyen Âge, læss, analyses archéométriques, alluvions fluviatiles, étude de provenance, Bruxelles.*

1. Introduction and Historical context

As many clay types are present in Belgium, bricks were widely used in construction, often in concurrence locally with stone, due to local availability and because the price of building material is strongly influenced by the distance of transport. Paleozoic and Mesozoic quartzites, slates, limestones, and sandstones are primarily available in the Walloon region (the southern half of Belgium). Building stones from the Brussels-Capital and the Flemish regions (the northern half of Belgium), are restricted to rare occurrences and small volumes. They are Tertiary in age, for instance the pale yellow sandstones of Brussels (in particular the calcareous facies of Gobertange), the Balegem stone (= Lede stone, the most important historical building stones in the ancient county of Flanders during the 15th and the 16th centuries and also exported on a large scale to Zeeland and Holland, The Netherlands), iron-cemented sandstones, and quartzarenites (Dreesen *et al.*, 2003; Dreesen & Dusar, 2004). Beside these local sources, other varieties of stones were imported and bricks were produced in Brussels and/or imported. Furthermore, urban demographic growth and the need to build "quickly" at lower cost, ensured that bricks were massively used. Several archaeometrical studies of brick production in different European countries have been published recently (e.g. Kristály *et al.*, 2011; López-Arce *et al.*, 2003; Wijffels, 2004; Wolf, 2002), however, no such study of historical Belgian bricks Belgium has been published.

Raw material for brick making occurs in every Belgian province and most major cities and villages were probably supplied by either adjacent brickyards or brick transported from neighboring localities. While bricks have been used in Belgium since Roman times, mediaeval bricks first appear in NW Europe during the 10th century (Sapin *et al.*, 2008; Blain, 2011) and are more common from the second half of the 12th century. However, they were first produced in the county of Flanders from the early 13th century on. Another innovation of the Middle Ages is that low-grade, more coarse-grained clays were used to manufacture bricks (Arntz, 1971; Hus *et al.*, 2003).

Brick is one of the main materials used in architectural production in the city of Brussels and the whole of the former Duchy of Brabant. During the 13th century Brussels was essentially made of wood, earth and stone, but the adoption of brick at the end of the 13th century profoundly changed building methods and shaped the face of the city as we know it today. The local production of bricks is attested through various ordinances promulgated by the city and other archival sources (production accounts, legal acts of renting or donations of land in order to extract brick earth…) (Sosnowska, 2013, 2014). In the 16th and 17th centuries, brick became the material *par excellence* of Brussels architecture. Alongside local production, the Brussels construction sector made considerable use of foreign building materials. The first authorization to import bricks, which goes hand in hand with that of lime, dates back to 1551 (Martiny, 1992, p. 20), about ten years before the completion of the Willebroek Canal, linking Brussels to the Rupel, then to the Scheldt and Antwerp, allowing boats to trade with the territories north of the capital and to avoid sailing on the capricious course of the Senne.

However, the extent of brick trade over time remains difficult to assess due to a lack of an adequate analysis of various archive collections, which – until now – only recorded this type of product with certainty at the end of the 17th century. This period corresponds to an intense phase of reconstruction following the bombardment of the city by the armies of Louis XIV in August 1695, which devastated the central parts of the city around the Grand-Place (Sosnowska & Goemaere, 2016). A major part of the city centre was rebuilt in three to four years requiring a colossal quantity

of building material partly imported from the well-known Boom brickworks (Belgium, province of Anvers) (Culot *et al.*, 1992), and from the Netherlands. It can be assumed that the massive importation of foreign bricks met an exceptional demand, and that Brussels brickmakers were unable to sufficiently supply the numerous construction sites in this limited period of time (Sosnowska & Goemaere, 2016). The city provided a designated area for citizens to put all the rubble resulting from the bombing but this proved insufficient. The magistrate obliged everyone to put all waste on their own property, and as a result, we found many recycled bricks and stones in rebuilt houses. It was not until the second half of the 18th century that a large supply of "foreign" bricks appeared again, attesting once more to a lack of sufficient local brick production at the time of the construction of the Palace of Charles of Lorraine, which replaced the old ducal residence. In order to not delay construction, an order for more than 1,000,000 bricks was placed at the brickworks of Rupelmonde, located on the left bank of the Scheldt at the confluence of the Rupel River (Waucquez, 2013).

It is not easy to reconstruct the Brussels brick industry of the Ancien Régime (Sosnowska, 2013). The destruction of the City's archives in 1695 caused an irremediable loss of information. No material traces of brickworks have been found within the framework of this research, with the exception of very incomplete remains of one or more kilns at the convent of Pauvres-Claires (unpublished data provided by B. Claes). The oldest extent written and iconographic sources date back to the 14th century and allow us to locate certain brick kilns more or less precisely in the same district as lime kilns (Henne & Wauters, 1845). These are located opposite the Grand Béguinage, between the Senne and the present rue de Laeken, on land situated in the alluvial plain of the Senne. The same is observed in the case of land used for brick earth extraction, notably that of an orchard at the Driesmolen (figures 1, 9) exploited for this purpose between 1447 and 1450 by Jean Van Ruysbroeck, master builder of the Town Hall tower from 1449 (Dikstein-Bernard, 2007). The production of bricks is also attested for the construction of the church of the Rouge-Cloître. Prior Daneels ordered the firing of 36,000 bricks in 1381 and 100,000 in 1383 (Halkin *et al.*, 1970). These two examples demonstrate the production of different brickworks from the 14th century onwards. These intra muros brickworks contradict the classic model of brickworks always being situated on land outside of the city. This model is based on three arguments: the cost of the installation, which requires large areas of land, the relative danger of these installations, and the pollution they cause (Sosson, 2000). The city of Brussels did not definitively prohibit the installation of intra muros brickworks until the 18th century (Martiny, 1992). The enclosure that surrounded the city of Brussels encompassed vast undeveloped grounds, as the plans drawn in the 16th century by Deventer (1550), Braun and Hogenberg (1572) and in 1649 by Blaeu (Danckaert, 1989, 38-39) testify. The contract concluded between Faye and the city of Brussels, allowing the installation of brickworks on the so-called Béguines meadow, confirms production within the city limits, at a location away from the densely populated roads of the city, which avoided the risk of fire propagation (Balestracci, 2000).

The archives relate the existence of brickworks from the 15th century to the 18th century outside the city walls, either directly on the outskirts of the second urban enclosure, or in the suburbs close to the city. In most cases, the brickworks were located not far from the city gates to facilitate the transport of products. The sites mentioned are located on or near major traffic routes: the Senne, the current rue de Laeken (figure 1, points 1 and 2), chaussée d'Ixelles (figure 4), chaussée de Wavre (figure 1, points 5, 6), chaussée de Mons (figure 1, point 8), and Porte de Flandre (Steenweg) (figure 1, point 11); or country roads (figure 1, points 5, 12). Transport and communication routes appear to be essential for the location of these industries, as demonstrated for the Netherlands by Hollestelle (1961). Access to water is another important factor. Three brickworks were located along the Senne (figure 1, points 1, 2 and 13). One (figure 1, points 11) was probably located not far from the Senne cut-off (Guillaume & Meganck, 2007). The factory on the heights of Obbrussel (figure 1, points 5) was supplied with water from the Elsbeek and was located near sand pits exploited since the Middle Ages on the current territory of Saint-Gilles (Guillaume & Meganck, 2004-2012). The "Eggevoorde" brickworks were likely fed by the Maelbeek stream on its border (figure 1, points 5, 6), and the brickworks supplying the Rouge-Cloître by the Blankedelle (figure 1, points 14).

Few studies have attempted to determine the source of bricks. Gurcke (1987) provides a comprehensive overview of previous work where bricks have been useful in archaeology. It is often assumed that ceramic building materials such as bricks and roof tiles were made of local raw materials and were not transported over significant distances. But it has sometimes proved to be incorrect as in the case of Roman roof tiles, which may have been shipped between different parts of the empire. The aim of our research is to give a mineralogical–petrographical-chemical characterization of the historic bricks made in Brussels and its periphery,

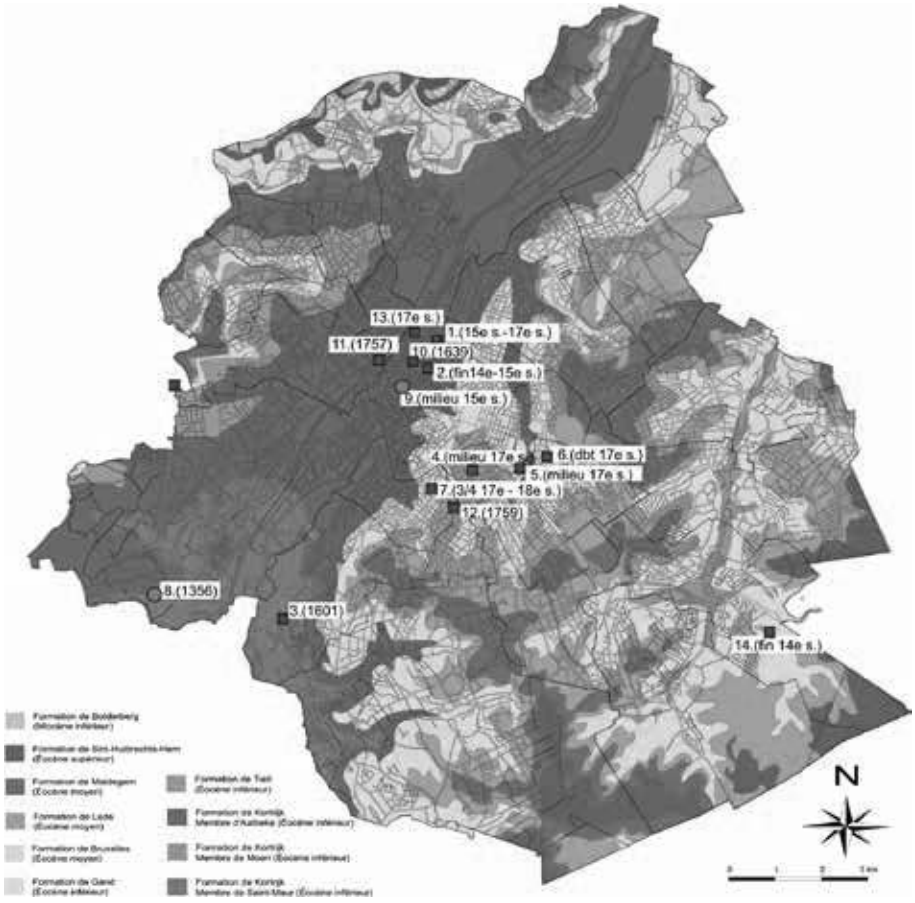

Figure 1: (See color plate ••) Geological plan of the Brussels region with locations of brickyards (in red) and clay extraction sites (in orange) mentioned in the archives. (Map : Buffel e.a.; DAO: C. Ortigosa & P. Sosnowska © DMS-ULB).

Figure 1 : (Voir planche couleur ••) Carte géologique de la Région de Bruxelles-Capitale situant les différentes briqueteries (en rouge) et les sites d'extraction d'argiles (en orange) trouvés dans les archives. (Plan : Buffel e.a. ; DAO : C. Ortigosa & P. Sosnowska © DMS-ULB).

determine provenance and sources of raw materials ("clays" and moulding sand). Fired clay bricks locally produced in Brussels will be referred to as "bricks" hereafter.

2. Geographical and geological context

The NE-oriented valley of the Sambre and middle Meuse ENE-trending valley (figure 2) separate two distinct physiographic Belgian domains. To the north of this axis, the southern low plateau area of Middle Belgium (elevations between 100-200 m) is composed of, from west to east, the Hainaut, Brabant and Hesbaye plateaus. It displays a slightly WNW-sloping topography. To the north, these low plateaus give way to similarly sloping dissected interfluves that separate regularly spaced linear NNE-trending valleys and end in an irregular gentle slope leading northward from 50 to 20 m altitude. Brussels-city is situated in the Senne alluvial plain. The Pleistocene and Holocene sedimentary infilling of the Senne alluvial plain is made of gravels, sands, loams, clays, peats and slope deposits. The city is crossed by the 103 km long (around 55 km long before its entrance in the Brussels-Region) S-N flowing Senne River, and is part of the Scheldt fluvial hydrological basin. Brussels Region is part of the Brabant plateau covered by thick quaternary loess deposits, lying on thick series of sub-horizontal Eocene and Oligocene marine and continental sands and clays, which are sometimes rich in glauconite and small amounts of sand-sized angular fragments of flints (reworked after Cretaceous deposits), Cretaceous chalks and a Lower Palaeozoic folded and faulted basement. For supplementary geological information, see Buffel & Matthijs (2002), De Maeyer *et al.* (2012) and Devleeshouwer & Pourriel (2005/2006). In the Brussels-Capital Region, the river was almost entirely covered during the 19th century, and numerous works have strongly modified the topography including the infilling of some tributaries. The Brussels-Capital Region, an area of 162 km^2, has been an autonomous Belgian region since the 1989 regrouping of 19 old communes as Brussels-city, Auderghem, and Uccle. The city developed outwards starting from the fortified medieval city centre encompassing suburban villages and farms. The population of approximately 20,000 people during the 14th century has grown to around 1.2 million inhabitants currently.

Figure 2: Geographical map of Belgium and the Netherlands with cities (in red) mentioned in the text indicated (DAO: N. Bloch © ULB).

Figure 2 : Carte géographique de la Belgique et des Pays-Bas localisant les différents lieux (en rouge) mentionnés dans cet article (DAO : N. Bloch © ULB).

3. Material & methods

The corpus (table 1) includes material from the collection of architectural ceramics kept at the archaeological repository of the Directorate of Monuments and Sites of the Brussels Regional Public Service, mainly from numerous preventive archaeological operations carried out in the Brussels region. Additional fieldwork was conducted to collect as much data as possible and to take new samples. New sites have been added to the corpus from excavations carried out by the Archaeological Heritage Department and by approved operators. Buildings well dated by dendrochronology, archaeology or written documentation (construction accounts…) were primarily selected. The studied buildings are mainly located in the city centre, rather than the outskirts of Brussels. The entire architectural spectrum was investigated: modest and bourgeois settlements, urban palaces, religious, civil and military monuments and agricultural buildings. Depending on the nature of excavations, the quantity of samples varied greatly, from a few cubic centimetres in protected masonries to the collection of several dozen complete bricks. The corpus covers a period stretching from the end of the Middle Ages (late 13th century) to the end of Modern Times (c. 1875). This last period constitutes a phase of profound transformation in Brussels brick production, as well as the change in brick formats and firing methods.

Macroscopic descriptive criteria including formats, colour, overall appearance and matrix, traces of shaping, and weight were recorded for all bricks. The size of a brick is usually the main characteristic highlighted by the archaeologist when describing masonry and is indeed an essential element to distinguish different construction periods. This approach is particularly obvious when two masonries are well differentiated. For example, bricks produced in the 13th and 17th centuries in Ypres (former county of Flanders), differ by up to 10 cm, gradually decreasing in size (Dewilde, 2008). In our study, 25 to 50 bricks were measured per masonry. Intervention (renovation of the edifice, classified or protected building) does not always allow for the same number of measurements as for a building that is to be demolished. In practice, less than 10 bricks were measured in unfavourable cases while in other cases, 800 bricks were examined.

Physical and chemical sciences applied to products of the clay industries allow investigating ceramic technologies, provenance, sources of raw materials and trade/exchange patterns (Dunham, 1992; Pavía & Roundtree, 2005; Pavía, 2006). No data exists for Belgian bricks, furthermore (geo)chemical and mineralogical data are rare in the Belgian literature, except for the Boom clay (Laenen, 1997; Vandenberghe *et al.*, 2014). The Boom clay (Rupelian, Early Oligocene) has been exploited along the Rupel and Scheldt rivers since the 13th century for brick making and at times for roof tile fabrication and more recently for the expanded

Briques faites à Bruxelles									
Ref.	ID	US	N°	Adresse/Address (Bruxelles)	Age	Hydromorphie	Couleur de la pâte	Pâte	Type
PS-5	BR81	US0258	00001	Tour Annessens	15e	forte, ooïde, racine	rose saumon	silteuse	A
PS-8	BRU-06	US0004	00002	Grand-Place, 15 ('t kelderke)	1441	forte	rouge violacé	silto-sableuse	A
PS-14	BRU-88	US'0036		Rue de l'Escalier, 36	15e s.	forte	rouge violacé	silto-sableuse	A
PS-15	BR-274	US'0202		rue de Flandre, 5	16e s.?	non	rouge homogène	silteuse	B
PS-17	BR274	US0401	00005	rue de Flandre, 5	16e s.?	oui	orange sombre	silteuse	A
PS-18	BR274	US0401	00004	rue de Flandre, 5	17e s.	non	rouge clair	silteuse assez grossière	B
PS-19	BR-283	US0015		rue des Bouchers, 59	AR	forte	rouge brun	silteuse	A
PS-23	BR-283	US0002	00001	rue des Bouchers, 59	AR	non	orange à zones claires	silteuse homogène	B
PS-24	BR-263	0004		rue de Laeken, 120	16e s.	oui	rouge un peu violacée	silteuse	A
PS-25	BR-283	0006		rue des Bouchers, 59	AR	non	orange clair	sable très fin/silt grossier	B
PS-26	BR-274	0401	00004	rue de Flandre, 5	16e s.?	oui	orange-rouge	silt sableux	A
PS-27	UC01-02	US433		Uccle - place Saint-Job/château Carloo	1770	non	rose clair	silteuse fine	B
PS-28	UC025	US0004	00006	Uccle - avenue de Fré, 48/Ferme Rose	1648d	non	orange vif	silto-sableuse	B
PS-29	BR159	US3044	00050	rue Notre-Dame du Sommeil, 11-17	2/2 17e s.	non	orange rouge	silteuse fine	B
PS-30	BR100	US0090		ancien couvent des Pauvres-Claires	17e-18e s.	oui	rose	silteuse	A
PS-33	BR100	US1115		ancien couvent des Pauvres-Claires	4/4 14e-1/4 15e s.	oui	orange	silteuse	A
PS-35	BR017	US2029	00021	rue des Chartreux	15e-17e s.	oui	orange clair - beige	silteuse fine	A
PS-40	BR082/S01	US0046	00001	Tour Noire	?	forte	brun clair	silteuse fine	A
PS-42	BR053/S02	US0186	00001	îlot Saint-Géry / Sarma	15e-17e s.	oui	rouge orange	silteuse fine	A
PS-44	BR100	kapelmuur staal 4		ancien couvent des Pauvres-Claires	fin 15e - dbt 16e s.	oui	orange	silteuse fine	A
PS-45	BR211	US3068	00001-1	quai aux Bois-de-Construction, 3	1/2 17e s.	non	orange	silteuse	B
PS-47	AU004	US1343	00001	Auderghem - prieuré du Rouge-Cloître	17e s.	non	orange	silteuse	B
PS-48	BR159	US3160	00026	rue Notre-Dame du Sommeil, 11-17	15e-16e s.	oui	orange pâle	silteuse	A
PS-50	BR100	US0071		ancien couvent des Pauvres-Claires	4/4 14e-1/2 15e s.	oui	rouge	silto-sableuse	A
PS-51	BR115	US1049	00002	rue du Chevreuil, 19	ca 1775	oui	rouge foncé	silteuse	B
PS-52	BR100	US0160		ancien couvent des Pauvres-Claires	4/4 14e-1/4 15e s.	oui	orange	silteuse	A
PS-53	BR100	US0542		ancien couvent des Pauvres-Claires	1/2 15e - 1/2 16e s.	non	orange rouge	silteuse	B
PS-54	BR100	US0685		ancien couvent des Pauvres-Claires	1/2 15e - 1/2 16e s.	oui	orange rouge	silteuse	A
PS-56	BR	US0017	00001	rue des Chapeliers	1695-1700	non	orange	silteuse grossière	B
PS-58	BR029	--		Porte de Hall/barbacane d'entrée	3/4 14e s.	oui	orange rouge	silto-sableuse	A
PS-59	BR066	--		Palais du Coudenberg-Aula Magna	milieu 15e s.	oui	orange rouge	silteuse	A

Table 1: List and origin of bricks made in Brussels.
Tableau 1 : Liste et origine des briques produites à Bruxelles.

clay industry (Mertens *et al.*, 2003). Analytical techniques including petrographic microscopy, X-ray diffractometry (XRD) and Laser Ablation Inductively Coupled Plasma Mass Spectrometry (LA-ICP-MS) were used to study bricks (n = 75) made in Brussels and compare them with natural clays and archaeological materials (raw clays found in ceramic ovens and ceramics).

Optical petrography (OP)

Petrographic techniques are now applied to the investigation of a wide range of construction geomaterials, most notably building stones, aggregates, concrete and mortars (Ingham, 2011). However, the use of petrography to study kiln-fired clay bricks, tiles and architectural terracotta remains uncommon in the literature. Standard (45 × 35 mm) petrographic thin sections were made from 69 samples of bricks including 30 bricks made in Brussels. The sections were examined using a Nikon Optiphot-Pol polarizing petrographic microscope and standard petrographic techniques. The grain size of the inclusions was determined after the Wentworth grain size scale.

Scanning electron microscopy (SEM) – energy dispersive X-ray spectroscopy (EDS)

We selected bricks that represent the extremes of appearance for SEM (FEI Quanta 200, 23 kV, spot size 6-7) analysis to determine the relationships between inclusions and bulk clay, the composition of inclusions, the textural and microstructural features, the evolution of vitrification and to identify the secondary minerals observed in thin sections (interaction with the masonry lime mortar). Sawed fragments were mounted in epoxy resin and silicon carbide-polished (1200 mesh). Uncoated polished sections were examined using EDS spectroscopy (EDAX: Apollo 10 SDD silicon drift detector) at the Mineralogical laboratory of the Geological Survey of Belgium (GSB).

Laser Ablation Inductively Coupled Plasma Mass Spectrometry (LA-ICP-MS)

Analyses of brick samples were run at the Field Museum Elemental Analysis Facility (EAF), first between March and May of 2013 (samples PS-02 to PS-67), and then during February and March of 2017 (samples PS-72 to PS-78). The 2013 analyses were performed using an Analytik Jena (formerly Varian) Quadrupole ICP-MS. In late 2015, the EAF replaced its Bruker ICP-MS with a new Thermo ICAP Q ICP-MS. Details of the EAF instrumentation and methods have been published elsewhere (Druc *et al.*, 2017; Golitko *et al.*, 2016), and will be only briefly mentioned here. All samples were ablated using the same NewWave UP213 Nd:YAG laser system. Ablation was performed in a helium atmosphere with a gas flow rate of 0.50 l/min, with a laser output of 0.2 mJ and a pulse frequency of 15 Hz. Five or six brick samples were analyzed at a time, with two Standard Reference Materials (SRMs), NIST610 glass and NIST679 clay, ablated between each batch of samples. Additionally, New Ohio Red Clay (NORC) (Kuleff and Djingova, 1998) was analyzed before and after each batch of samples as a quality assurance standard. Ten 100 µm craters were ablated on each sample and five on each SRM. Both ICP-MS instruments were run in peak jumping mode, with three scans of the measured mass range per replicate, and nine replicates per ablation. The first three of these replicates were subsequently removed before calculating an averaging elemental signal strength (c/s) in order to account for surface contamination and to allow signal stabilization. Isotopes of 58 major, minor, and trace elements ranging from Li to U were measured, although several (P, Cl, As, Se, Ag, Cd, In, Sb, Bi) were removed from subsequent analysis due to low measurement precision resulting from extremely low concentration and/or inefficient ionization. Signal strengths were averaged across replicates and normalized to the corresponding silica signal strength to account for variability in ablation efficiency. After despiking data to remove anomalous values resulting from partial ablation of larger mineral inclusions (Golitko & Dussubieux, 2016), averaged and normalized signal strengths were converted to ppm elemental concentration values by a linear regression against signal values for NIST610 and NIST679 using certified or published values (Glascock & Anderson 1993; Grave *et al.*, 2005; Jochum *et al.* 2011; Meloni *et al.*, 1999) via the sum-normalization procedure described by Gratuze *et al.* (2001) and Speakman and Neff (2005). Comparison of measurements for NORC indicates no significant difference in elemental measurements across the two instruments utilized in this study. For NORC and samples, precision was on the order of 5% for major elements, and ranged between 10%-20% for trace elements (see Golitko 2011, 2015; Golitko and Dussubieux 2016). Geochemical analyses were performed on paste, avoiding visible inclusions, to identify clay provenance. No global public geochemical database exists in Belgium, and there are no raw clays available from workshops and kilns from Brussels. Therefore it is necessary to compare with different clayey/silty rocks coming from a large range of stratigraphical levels and geological environments present in the Brussels region. We used data from several different sources: the database esta-

blished by Golitko (2010) during his PhD research, new data performed on tertiary marine clays sampled from boreholes managed by the Geological Survey of Belgium (some coming from the Brussels Region) and other archaeometric studies. All samples were analyzed by the same laboratory allowing the comparison with the bricks of Brussels. Around 150 references samples were analyzed, ranging from Silurian weathered shales to Belgian Quaternary loess, complimented by Neolithic, Gallo-Roman, and Medieval ceramics and clays from potter's workshops.

X-ray diffraction (XRD)

The silty reddish matrix of the brick samples (n = 29) was reduced in size using a hammer and steel plate (wrapped inside paper to reduce contamination) then crushed using a Fritsch Laboratory Planetary Mono Mill. The powder was homogenized and ground by agate grinding balls in a grinding bowl. Afterwards the powder was passed through a 53 µm sieve. The remaining fraction was crushed again until the crystallites were all below 53 µm. Lime mortars were analysed separately. The powder was then loaded into stainless steel sample holders using back loading. Disoriented powder X-ray diffraction analyses were performed using a PANanalytical Empyrean diffractometer (Cu anode, Ni filter, 40 mA and 45 KV, 6 to 70°2Θ) and the semi-quantitatively interpreted using Visual Crystal 6 software (GSB laboratory). Percentages of minerals obtained through XRD analysis should be seen as estimates, as no internal standards were used. They are based on the relative proportions of the area under the curve combined with the RIR (Reference Intensity Ratio) value of different minerals. The presence of other minerals in quantities under a few % cannot be excluded using only this technique.

Magnetic susceptibility (MS)

The Kappabridge MFK1-A station (equipped with a CS-3 High Temperature Furnace and a CSL Low Temperature Cryostat module) at the GSB allowed measuring magnetic susceptibility parameters on small samples with a fully automatized system. This method is non-destructive for the samples, and complementary to other analytical tools. The magnetic susceptibility of 35 brick fragments was measured. The mean value of each object was calculated from three measurements. For individual bricks, the values differed from less than $1x10^{-8}$ m^3/Kg and the instrumental deviation was below this same value during all the analyses.

4. How to recognize a brick made in Brussels?

The bricks display typical features of hand-moulding including low variability in size, colours ranging between orange and deep red, uneven surfaces and edges, and moulding striae. Hardness and cohesion vary widely as a function of firing temperature.

Formats

In Brussels, there is no obvious distinction between bricks produced in the 14th and 18th centuries. Cabuy & Degré (1993) note that the format in use in Brussels between the 15th and the end of the 17th century measured 27 × 12.5 × 5.5 cm. Their finding must be taken with caution because it does not concern 14th and 18th centuries brick production and some archaeological studies, including the one carried out at the Hal Gate (last gate of the second urban wall), where a variability of the formats could be revealed. However, the differences between recorded dimensions are small (1-2 cm) (De Waha & De Poorter, 1993). This trend has been confirmed during other excavations conducted since the 1990s (Fourny, 1994a, 1994b; De Poorter, 1995; Diekmann, 1997; Blanquart, 2001; Massart, 2001; Demeter & Sosnowska, 2007). Our results show that between the 14th and 16th centuries, the Brussels brick sizes range from 26-30 cm in length, 12-13,5 cm in width, and 5-6,5 cm (sometimes 7 cm) in thickness (format I) (table 2, figure 3). During the 14th century, and perhaps already since the end of the 13th century, smaller bricks may have been used in addition to this format. There are at least two other brick sizes, one of 24/25 x 11,5/12 x 4,5/5 cm (format III), the other 25/26 x 11/11,5 x 5/5,5 cm (format IV). If this hypothesis is confirmed, it would make it possible to affirm that in the 14th century Brussels brickworks produced bricks in a distinguishable format. But from the end of the 14th to the beginning of the 15th century on, these different products disappeared in favour of a single type of brick, a hypothesis which seems to be confirmed by the first Brussels production ordinances and the Ghent studies of brick production (Laleman & Stoops, 2008). This variability of the first type of bricks (type I) stabilizes around 26/28 x 12/13 x 5/6 cm from the turn of the 17th century until the last quarter of the 18th century, in contrast with the size reduction attested in the former county of Flanders (Lehouck, 2008; Coomans & van Royen, 2008; Debonne, 2008; Wets, 2008) and certain regions or cities in the current Netherlands (Hollestelle, 1961). Some questions remain. Can we interpret this variability as resulting from production carried out by two dif-

	Format cm (lxwxh)	Color (Munsell Soil Color Charts)		Datation
Local bricks format I	26/30x12/13.5x5/7	2.5YR4/6 to 7.5YR5/6	red to strong brown	14th c. to 16th c.
Local bricks format II	26/28x12/13x5/6	2.5YR5/8 to 5YR5/8	red to yellowish red	17th c. to 18th c.
Local bricks format III	24/25x11,5/12x4,5/5	2.5YR4/6 to 7.5YR5/6	red to strong brown	14th c.
Local bricks format IV	25/26x11/11,5x5/5,5	2.5YR4/6 to 7.5YR5/6	red to strong brown	14th c.

Table 2: Four groups of brick sizes used for the main structures in Brussels construction (modified after Sosnowska & Goemaere, 2016). lxwxh: length (cm) × width (cm) × height (cm).
Tableau 2 : Quatre groupes de dimensions de briques utilisées pour les constructions bruxelloises principales (modifié d'après Sosnowska et Goemaere, 2016). lxwxh : longueur (cm) × largeur (cm) × hauteur (cm).

ferent brick manufacturers during the same period? Does it result from the manufacturing process itself that includes two phases of clay shrinkage, one during drying, and the other during firing? Or is size variability chronological, allowing construction campaigns from distinct periods to be identified? The analysis of these results shows a general typo-chronological evolution of the bricks produced in Brussels.

Colours

Colour was defined using the Munsell Soil Color Charts directly on site or in the laboratory. Colours range between orange and deep red. The main objective of the "colourimetric" approach is to determine possible colour differences in local Brussels architectural production, which could indicate either changes in firing or recipe, or imported material. The colour of a brick depends on several raw material specific factors, including the initial mineralogical composition of the clay and its homogeneity, the presence of organic compounds, the mineralogical composition of the fired-brick, the percentage of calcium carbonate and the iron content. Extrinsic factors are temperature, firing time, time during which a constant temperature was maintained, and oxidizing or reducing conditions during firing and cooling (Firman, 1994; Viaene *et al*., 1996), but also the position of the brick in the kiln and the type of combustibles utilized. The interior colour of a brick may differ from that of its surface if these parameters vary between the surface and the core of the brick, but also from the presence of iron or organic matter-rich spots. Some bricks have a "black" core resulting from incomplete oxidation of iron in the centre of the brick and the presence of sulphur or carbon in the raw clay, but also from an overly dense mixture, or overly fast drying or firing. These three factors prevent the circulation of oxygen through the brick and thus generate oxidation only on the surface of the brick (Firman & Firman, 1967).

Figure 3: (See color plate ••) Two examples of brick formats commonly used in the city of Brussels from the fourteenth to the eighteenth century. Below: fifteenth century. Top: second half of the eighteenth century.
Figure 3 : (Voir planche couleur ••) Deux exemples de formats de briques communément utilisés dans la ville de Bruxelles du XIVe siècle au XVIIIe siècle. En bas : XVe siècle. En haut : seconde moitié du XVIIIe siècle.

Matrix

Macroscopic observation shows silty matrices, sometimes slightly micaceous, the presence of residual stratification and deformation during moulding, clay-rich and iron-rich subrounded inclusions and macroporosity. The shape, granulometry and percentage of inclusions present in each brick were also estimated. Only megapores and macropores, up to 5-7% of the volume, can be visually estimated and quantified. Other pore types require microscopy and laboratory measurements. The observed porosity results from various factors: air bubbles trapped in the brick when wor-

king the clay, tubular impressions from carbonized plant debris, but also shrinkage due to the departure of different types of water during drying and firing. Macroporosity and occasional cracks are also distinctive features. Bricks are characterized by their porosity and large size, which remains relatively stable from the 14th to the 18th century (Sosnowska, 2013; Sosnowska & Goemaere, 2016). After polishing the sawed surfaces, it was possible to distinguish in between two different end-members groups of bricks, respectively called type-A and type-B (figure 4).

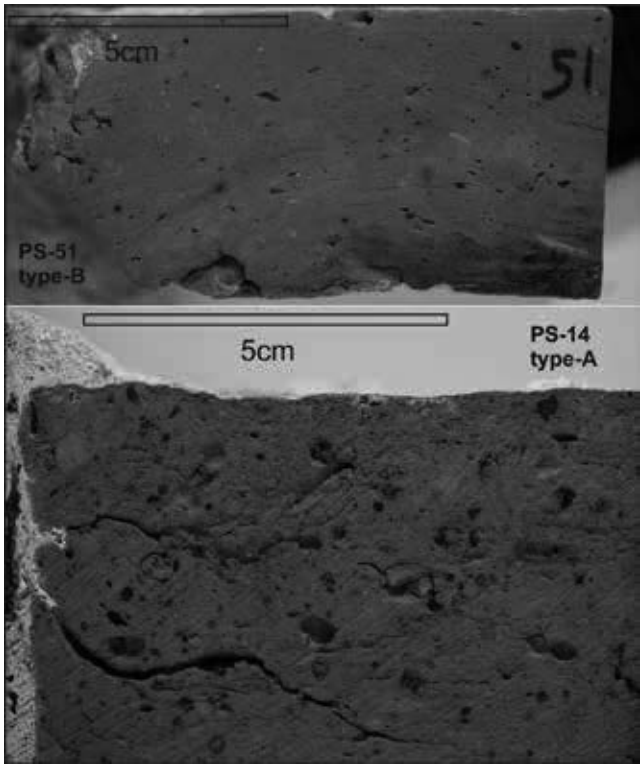

Figure 4: (See color plate ••) Cross-sections of the two identified brick types. Upper picture: brick of type-B (ref. PS-51) showing a silty orange-red matrix with thin streaks with clearer tones (residual traces of the stratification plane in the raw material), and megapores and macropores. In the right lower part, the blackish zone represents localized overfiring and the beginning of melting. Lower picture: brick of type-A (ref. PS-14) rich in iron-rich brownish inclusions and clay-rich inclusions, all surrounded by ring voids, and large pores with irregular cracks. A milky lime-mortar (left border) is made of lime and sand-sized quartz grains. Traces of sawing are due to the relative softness of the brick and lack of resin-infusion.

Figure 4 : (Voir planche couleur ••) Coupes à travers les deux types de briques. Image supérieure : brique de type B (réf. PS-51) montrant la matrice silteuse rouge orange avec de fines traces plus claires (fantômes du plan de stratification de la matière première), les mégapores et les macropores. La partie inférieure droite, plus sombre, représente une surcuisson et le début de la vitrification. Image inférieure : brique de type A (réf. PS-14) riche en inclusions ferriques brunâtres et en inclusions argileuses, soulignées par des pores les contournant ainsi qu'une porosité élevée et des fractures irrégulières. Un mortier laiteux (bord gauche) est constitué de chaux et de sable quartzeux. Les traces de sciage sont dues à la friabilité de la brique et le non recours à des résines pour consolider le matériau.

Type-A corresponds to the oldest bricks. The colour is red to strong brown. It is made of a homogeneous silty loam, sometimes finer, sometimes a little bit sandy (very fine-grained sands). The sediment is very weakly stratified even in thin section. The matrix shows occurrences of dark red to black-brown millimetre-sized ferric patches or spots, iron-rich glaebules, very rare grogs and rounded orange to red semi-plastic clayey inclusions, lighter in colour. Iron-rich glaebules are similar to pedogenic features present in gley/pseudogley soils (see the following chapters regarding petrography and sourcing). We can distinguish colour mottles, defined as glaebules with diffuse boundaries, nodules and concretions which have fairly well defined smooth to irregular boundaries. Nodules have no internal structure, whereas concretions have concentric banding indicative of periodic addition of material of different composition or texture. Septaria are nodules or concretions with radiating and concentric cracks resulting from shrinkage or hydraulic fracturing in the raw material, but also due to the firing of the paste, resulting in the transformation of iron hydroxides to hematite. The thermally induced transformation of goethite (α-FeOOH) into hematite (α-Fe_2O_3) occurs at about 300°C (Gialanella *et al.*, 2010).

Type-B is characterized by a more homogeneous orange cadmium-coloured matrix and the (quasi) absence of brown ferric spots or clay inclusions. It is made of a homogeneous silty loam similar to type-A. Under the binocular, it's possible to recognize very small (<0.5 mm) thin and shiny white mica flakes. The colour is generally homogeneous (orange-cadmium to light red) but lighter colours occur at some places. The bricks are "tender". The material seems to be homogeneous to the naked-eye. Polished sections of the two types show relics of the initial stratification planes from the raw clayey material deformed during brick shaping. Sometimes, the stratification is underlined by ultra-thin layers of medium-grained quartzose sand (monocristalline quartz and rare flint grains).

Both types show fine moulding sands on the brick surfaces. Additionally, a lime mortar is bound to the brick in some samples. External moulding and straw prints can sometimes be observed on the surface but especially in the paste and in various proportions. Concerning the addition of degreaser in the paste, the Brussels archives related to the production of bricks, remain difficult to interpret. The cost and profit account for the production of a brick fac-

tory, dated 1433, indicates the purchase of straw and sand. Nevertheless, it cannot be concluded that this proves the use of these components as degreaser. Indeed, these two components are used during the shaping of the bricks and in some cases during the drying phase, as an insulating cover placed on the ground to protect the bricks.

5. Analytical results

Brick Petrography (OP & MEB/EDS)

As for ceramics studied in thin section, the fabric of archaeological fired clay bricks consists of the paste constituted by clay matrix and particulate inclusions and voids. Ceramic building materials differ from pottery because they are made from relatively coarse-grained and poorly processed clay. Brussels bricks contain a high proportion of non-plastic material. They are made of silty loam with clays and a smaller amount of sand. Their composition is about 25/70/5% clay/silt/sand, respectively. These proportions vary from one brick to another one but the silt fraction is always the main granulometric fraction. A summary of the main optical mineralogy results is provided in table 3.

The matrix is not translucent because of iron staining. Petrography identifies changes in the ceramic fabric due to firing, suggesting relatively low temperatures (porous slightly birefringent matrix) in some cases, and high temperatures (opaque and isotropic matrix with a low porosity) in others. Furthermore, in well-fired, vitrified bricks, iron is combined with clay minerals and minerals are not resolved as a result. Minute plate-like crystals of phyllosilicates are only observed in the iron-poorest bricks, bricks heated to relatively low temperatures, or along the thinnest border of the thin sections. The colour of the clay matrix varies from one thin section to another from yellow-orange to red based on the interplay of three main factors: the abundance of Fe^{3+}, the richness of clay particles, and firing temperature. Red spots in the fired brick correspond to higher concentrations of iron. Distinguishing anthropogenic and natural compositional variation in clay-bricks is important for both provenance interpretation and the reconstruction of manufacturing technology. The type-B bricks show a homogenous matrix while in type-A bricks, microscopic heterogeneity in the clay matrix derives from the use of variegated clays with fine-scale variation in the laminated sedimentary raw material source. This stratification is due to very small granulometric variations but also the alignment of micro-flakes. Mica macro-flakes in the coarse silty or sandy fractions never show concentrations along peculiar planes. Sometimes, one-sheet layers of quartz sand-grains occur. This micro-stratification indicates the absence of homogenization before the brick was formed. Additional deformation is also observed near the external borders of the brick due to the clay being forced into a (wooden) mould. The "clay" has been dug and used more or less in its natural outcropped state. In between the two end-groups, the micro-stratification is a relic. In the type-A group of bricks, traces of bioturbation by animals (worms) and plants (roots) living in the upper layer of the soils and pedogenesis (argilans, cutans and iron-rich pedogenic nodules, spots and patches) are frequently observed in thin sections. Sometimes, small pockets filled by moulding sand are included in the paste as well as isolated, but rare, grains of quartz with the same granulometry as the moulding sand. Another influence on internal heterogeneity is the post-depositional "alteration" of the bricks. Soluble calcic minerals such as secondary calcite (from lime and quick lime mortar), gypsum and apatite may be precipitated within the pore system by infiltration and capillary waters in the masonry, altering the bulk material chemical composition. Pores can be fully filled with fibrous calcite with a fan-shape structure, and more rarely by anhedral crystals of secondary calcite. Calcareous fringes can be deposited on the interior surface of voids, and calcite is present as elongated micro-sparite dog-tooth crystals.

Particulate inclusions are mainly composed of a sandy fraction made of well-sorted fine-grained sand (125-250 μm). Quartz grains show bimodalism because there is a gap between quartz occurring in the silty fraction and fine-grained sand. Sand used to make minor adjustments to the quality of soil can be added to soil when drying to prevent the soil from becoming too brittle and can also be used as a stabilizer in a mixture. But in the case of the Brussels bricks, it could be due to primary stratification in the raw "clay" in the form of a thin alternation of silt-grained and fine-sand grained layers, then modified by pedogenic process and/or minimal paste preparation. Subrounded to subangular isometric grains of monocristalline quartz dominate the mineralogical assemblage. This morphology differs from those of tertiary sands where the majority of grains show an elongated or a triangular shape. Quartz often shows an undulatory extinction. Clasticity can reach 600 μm but coarse sand, very coarse sand, and gravel are never found in the paste. Polycristalline quartz, grains of flints, rounded glauconite, fresh and weathered feldspars as well as accessory minerals (heavy minerals) occur more rarely. Inclusions reflect a well matured sediment. Lithic fragments occur at very low concentration. Exceptionally, organic phosphatic grains are observed as well as infrequent detrital xenomorphic carbonated (micrite) inclusions, maximally 300 μm in length. The

	Paste							Pores
	75 to 85%							15 - 25%
	Clay-silt matrix (<10 µm)	Particulate inclusions (>10 µm)						
	10 to 30%	*70 to 90%*						
		Medium to coarse silts	Very very fine-grained sands (<75 µm)	Very fine sands (75-125 µm)	Fine sands (125-250 µm)	Medium sands (250-500 µm)	>500µm	
		>90%	<10%	<<1%	<1 - 5%	<<<1%	--	
Minerals and other petrographic features								
Quartz	xxx	xxxxx	xxxxx	(x)	xxxxxxx	(x)	--	
K-Feldspars	?	x	x	--	--	--	--	
Plagioclases	?	x	x	--	--	--	--	
Micas flakes	xxx	xx	x	(x)	x	(x)	--	
Glauconite	--	x	x	--	(x)	--	--	
Iron oxides (glaebules)	x	x	x	xx	xx	xxx	xxxxx – 0	xx
Pedogenic features	--	X – 0	X – 0	X – 0	X – 0	X – 0	(x)	
Heavy minerals	--	(x)	(x)	--	--	--	--	
Flint and cherts	--	(x)	(x)	--	(x)	(x)	--	
Rocks fragments	--	--	--	--	--	--	Rare (silicified sand)	
Bones	--	Very rare	Very rare	--	--	--	--	
Vegetal debris	--	--	--	--	--	--	Traces	Rare
fossils	--	--				Very rare (silicified)	Very rare (silicified)	
Recent fauna	--	--	--	--	--	--	--	
Primary calcite	--	--	--	--	--	--	--	--
2nd Calcite	--							
Legend:								
-- : absent; (x): rare; x: present; xx: frequent; xxx: abundant; >xxx : dominant; ?: undetermined								

Table 3: Main petrographic features observed by optical microscopy of bricks.
Tableau 3 : Caractéristiques pétrographiques principales des briques au microscope optique polarisant.

micritic aspect of these inclusions is probably due to firing at temperatures over 850°C (the temperature of calcite decomposition). These carbonates may originate from Tertiary or Cretaceous reworked layers. Their very low content does not affect the mechanical resistance of the bricks. Neither recent shells (bivalve molluscs or gastropods), nor algae were identified in thin sections. Detrital bioclasts are observed in a few thin sections as broken small straight or curved silica sponge spicules (microscleres), as well as one silicified nummulite (290 µm) and small fragments of bones. Siliceous bioclasts occur and had their primary source in the reworking of cretaceous and tertiary sediments. Rarely, natural temper (vegetal fragments) and accidental temper (moulding quartz, slag fragments) occur in the bricks. There is no addition of quartzose sand temper to the clay paste. Imprints of vegetal fragments were observed on the outer surfaces of bricks, but vegetal remains and moulds were not seen in the core of the bricks except in one case, where a charcoal particle had been impregnated by fine-grained iron oxides. This likely represents a piece of fuel accidentally incorporated during the moulding of the brick. Circular transversal sections of roots without any cellular structure preserved were observed

in some type-A bricks. No traces of coal dust or cinder were added to the paste to assist in firing.

All macro- and mesoscopic observations of the iron-glaebules in type-A bricks are corroborated at the microscopic scale. Nevertheless, we observe clastic grains inside the haloes and in the nodules and occasionally quartz grains show partial dissolution. Iron-stained clays are sometimes observed inside nodules. Iron richness is variable from one glaebule to another, and is highly variable within the same brick and from one brick to another. Concentrically layered glaebules show two or more thin haematitic laminae, or a haematitic nucleus, but numerous ferric glaebules have an internal undifferentiated fabric. The biggest glaebules are compound glaebules resulting from the coalescence of smaller glaebules and cementation by iron oxides. Note that compound calcite-ferric glaebules were not observed in thin sections. A more complete description is given below.

All bricks show a porosity ranging between micropores and megapores. Pores are rarely connected, reducing their permeability. The biggest pores are cracks or are linked to the thermal decomposition of vegetal fragments, but also to the Fe-rich spots. In general, smaller pores between clay particles disappear at higher firing temperatures as a result of melting and coalescence of particles, and larger pores form due to gas release caused by dehydroxylation (loss of OH^- groups) in phyllosilicates (Elert *et al.*, 2003). Additional porosity is attributed to the transformation of iron hydroxides occurring in the raw material into microporous iron oxides, which leads to a significant increase in porosity in the brick.

The clay is formed into a wedge shape and all sides are covered with a "releasing agent" which prevents the clay from sticking to the sides of the mould. The most common releasing agent is sand. It is useful to observe sand utilized in the brickmaking process to determine its source and distinguish local from non-local raw material. Moulding sand is composed of rounded non isometric quartz grains with rare grains of flint, feldspars, glauconite, small-sized forams (*Nummulites variolarius*) and lithic debris composed of sandy limestones. These characteristics link this sand to the Lede Formation (Lutetian, Eocene). Due to normal faults affecting its horizontal Tertiary layers, the sands of the Lede Formation outcrop in Brussels to the west in the Senne valley sides and are mined locally in open pits (see Camerman, 1955 for further information regarding extraction of this raw material in Brussels). Toponyms indicate the presence (and extraction) of sand—extraction on the rue des Sables (Suyvelstraet or Zavelstraet) dating back to the 13th century (Henne & Wauters, 1845, 434). The current Place du Grand Sablon takes its name from the Dutch "Groote Zavel", a space located outside the first urban enclosure dating from the 13th century. It refers to the existence of a "zavel poel" that can be translated as a swamp or pond with sand that was filled in 1615 (Henne & Wauters, 1845). A "plaine des Sables" is also mentioned in the hamlet of Saint-Gilles, on the outskirts of the town (Henne & Wauters, 1845,). Finally, an arm of the Senne called "Sennette au sable" is also mentioned several times (Henne & Wauters, 1845). The sale of sand is evident through analysis of the tolls to be paid at the gates of the city (Henne & Wauters, 1845). The few Brussels archives relating to the production of bricks mention the purchase of sand without however specifying its use, as is the case in a document issued by the Brussels City Council in 1433 (Sosnowska, 2013). The French treaties of the 18th century are more detailed. They underline its importance in the manufacturing process and precisely describe its use in the different phases of the chaîne opératoire and specify that all sand used in brickworks must be very fine. It was used in the preparation of clay, in the moulding and demoulding phase of the brick, during drying, when the bricks are placed on a sand-covered floor, but also in the manufacture of baking ovens, (Duhamel du Monceau, 1763).

Brick LA-ICP-MS

The chemical composition of archaeological ceramics is closely related to the chemical composition of the raw materials employed in their fabrication (Castro, 1999). The geochemical composition of the brick samples is given in tables 4 and 5. Bricks are silica-rich, indicative of a high quartz content silty matrix. Brick compositions show a close clustering in SiO_2 - Al_2O_3 - K_2O (figure 5) and SiO_2 - Al_2O_3 - (FeO+MgO) (figure 6) ternary diagrams (taken as examples), charactering a low variation in K_2O content. Bricks produced in Brussels, Auderghem and Uccle show similar chemical compositions for major, minor and trace elements, as shown through binary and ternary diagrams. The chemical compositions of the brick clay matrix are very similar and consequently, it is difficult to fully differentiate between the two petrographic groups regardless of the statistical methodology adopted. We observe partial cluster superposition indicative of small internal variations in the original sediments in addition to pedogenic processes of variable intensity. Comparison with the analyses of both geological and archaeological samples from our databases only shows good correspondence with quaternary loessic formations from the plateau and the walls of the Roman ceramic kiln at Asse (north of Brussels), which was built with local loessic material.

Samples	Be PS-05	Be PS-08	Be PS-14	Be PS-15	Be PS-17	Be PS-18	Be PS-19	Be PS-23	Be PS-24	Be PS-25	Be PS-26	Be PS-29	Be PS-30	Be PS-33	Be PS-35	Be PS-40	Be PS-42	Be PS-44	Be PS-45	Be PS-48	Be PS-50	Be PS-51	Be PS-52	Be PS-53	Be PS-54	Be PS-56	Be PS-58	Be PS-59	Uccle PS-27	Uccle PS-28	Auderghem PS-47
	type-A	type-A	type-A	type-B	type-A	type-B	type-A	type-B	type-A	type-B	type-A	type-B	type-A	type-A	type-A	type-A	type-A	type-A	type-A	type-B	type-A	type-B	type-A	type-A	type-B	type-B	type-A	type-A	? B	type-B	type-B
Major elements (%)																															
SiO_2	77.48	75.79	74.23	78.07	78.76	79.54	80.70	78.26	77.17	80.72	73.93	77.95	76.89	77.99	79.62	76.19	78.18	78.56	79.23	77.86	79.34	79.49	73.95	78.04	79.13	81.30	74.97	73.15	80.90	82.13	76.64
Al_2O_3	9.36	10.02	11.81	9.97	9.34	8.42	8.84	10.63	9.99	8.91	11.65	12.29	11.47	11.75	10.98	10.99	11.04	9.83	9.20	10.62	9.19	10.44	11.19	9.44	9.42	10.44	12.12	11.94	8.63	9.02	10.35
Fe_2O_3 tot	6.45	8.38	8.82	6.41	6.70	5.68	5.17	5.08	7.19	5.37	7.99	4.07	5.51	4.70	4.19	6.61	5.37	6.05	5.92	5.64	6.56	4.67	6.86	6.22	6.46	3.59	6.73	8.81	5.31	4.29	7.01
MgO	0.81	1.03	1.07	0.88	0.87	0.80	0.82	0.85	0.99	0.76	1.22	0.79	0.96	1.15	0.95	1.17	0.97	0.88	0.88	0.92	0.92	0.93	0.93	0.89	0.81	1.01	1.09	1.06	0.68	0.63	1.06
CaO	1.23	0.85	1.00	0.66	0.81	2.40	0.91	0.58	1.02	0.68	1.35	0.84	1.23	0.91	0.60	1.20	0.63	0.91	0.82	1.08	0.96	0.93	1.75	1.72	0.80	0.37	0.87	1.12	0.55	0.51	0.81
K_2O	2.21	2.06	1.58	2.33	1.88	1.68	2.04	1.92	1.96	2.05	1.94	2.80	2.58	2.20	2.21	2.08	2.09	1.74	1.92	2.14	1.46	2.18	2.61	1.91	1.96	2.19	2.51	2.27	2.25	2.34	2.31
Minor elements (%)																															
TiO_2	0.80	0.85	0.77	0.63	0.66	0.57	0.63	2.23	0.68	0.61	0.97	0.35	0.43	0.59	0.71	0.86	0.98	0.94	0.85	0.78	0.65	0.55	0.78	0.62	0.51	0.54	0.69	0.69	0.55	0.29	0.76
MnO	0.11	0.12	0.09	0.09	0.12	0.08	0.04	0.06	0.07	0.06	0.14	0.06	0.05	0.11	0.05	0.04	0.09	0.09	0.08	0.09	0.13	0.07	0.26	0.09	0.09	0.06	0.07	0.09	0.09	0.05	0.07
Na_2O	0.82	0.69	0.47	0.85	0.72	0.70	0.76	0.33	0.79	0.77	0.61	0.81	0.55	0.55	0.55	0.69	0.56	0.81	0.98	0.56	0.60	0.69	0.79	0.84	0.67	0.46	0.85	0.53	0.96	0.66	0.61
P_2O_5	0.74	0.21	0.17	0.10	0.14	0.13	0.09	0.05	0.14	0.07	0.21	0.05	0.32	0.04	0.14	0.18	0.10	0.18	0.10	0.31	0.20	0.05	0.88	0.23	0.15	0.04	0.11	0.34	0.09	0.08	0.39
(Major+Minor)/all elements (%)																															
	99.74	99.72	99.70	99.75	99.73	99.74	99.77	99.73	99.76	99.74	99.68	99.79	99.72	99.65	99.72	99.70	99.47	99.73	99.76	99.73	99.77	99.77	99.62	99.73	99.76	99.77	99.75	99.70	99.74	99.78	99.74
Trace elements (ppm)																															
Li	30.51	38.90	39.26	27.16	27.40	26.37	27.95	30.69	32.41	28.15	37.22	28.92	31.12	36.05	30.43	37.89	35.57	34.81	25.92	29.12	35.86	29.44	30.75	14.07	26.40	21.86	38.39	31.06	28.05	22.45	30.65
Be	1.87	2.22	3.38	2.11	1.73	1.63	1.74	2.01	1.82	1.73	2.70	2.89	2.29	2.19	1.95	1.99	2.38	1.79	1.87	1.91	1.79	2.07	2.18	2.08	1.86	1.75	1.97	2.71	1.82	1.68	2.02
B	58.89	43.89	48.43	26.98	42.12	46.32	45.74	43.75	47.86	43.51	48.76	45.67	35.20	49.93	37.98	43.94	50.19	47.51	37.01	43.15	32.47	57.58	36.16	20.64	42.08	103.74	41.22	45.30	61.90	33.70	46.94
Sc	11.13	11.81	15.79	10.79	10.69	9.02	10.01	14.71	11.59	10.86	17.89	10.54	11.82	16.92	14.79	13.74	13.46	11.85	11.50	13.87	11.12	12.42	14.60	11.56	11.19	11.46	12.72	14.18	8.36	8.29	13.74
V	81.25	99.55	109.79	90.16	69.32	82.85	66.24	99.41	85.20	94.80	101.34	71.57	90.54	90.14	81.01	87.96	94.53	78.71	87.66	88.73	76.00	87.81	82.14	78.10	75.82	83.37	78.45	87.74	84.61	54.03	77.53
Cr	80.07	80.14	108.18	70.01	77.11	65.73	67.46	72.59	87.13	68.27	93.14	52.70	94.69	79.11	69.79	96.49	79.04	76.49	55.83	80.98	72.16	64.23	70.81	104.09	75.55	67.89	90.39	82.10	71.18	51.14	116.74
Co	11.45	13.47	11.95	10.32	9.05	9.43	7.76	9.84	10.12	9.02	20.77	8.01	10.98	11.87	11.60	9.70	10.46	8.77	10.63	10.48	10.97	9.75	12.15	11.74	10.96	10.75	9.18	14.35	9.64	7.56	10.62
Ni	35.31	35.78	41.37	31.38	27.36	29.78	25.28	37.30	33.19	35.19	47.47	31.15	35.25	36.07	35.34	35.64	33.93	30.70	35.27	30.72	31.98	30.92	36.44	31.70	32.00	32.72	31.95	45.98	27.04	26.57	36.06
Cu	49.12	20.65	11.95	13.12	17.14	15.59	12.64	24.59	17.06	17.06	13.96	11.46	50.33	11.99	31.26	32.66	18.33	18.86	41.67	57.18	15.53	13.93	50.62	21.94	30.35	7.34	16.53	16.78	17.16	10.79	14.97
Zn	105.08	102.43	81.94	66.27	74.23	180.20	77.70	71.89	89.28	66.60	120.66	52.87	118.55	88.54	106.24	200.30	116.93	83.99	71.89	91.47	87.84	72.74	176.39	168.66	73.52	80.87	83.11	109.08	80.18	47.35	75.11
As	0.00	28.78	17.14	0.00	7.50	0.00	0.00	0.00	0.00	50.89	4.15	12.30	20.56	300.41	13.30	0.36	0.00	0.00	2.29	7.50	4.46	0.00	0.00	0.51	20.71	0.00	5.98	6.16	0.00	5.75	0.00
Se	0.00	0.00	0.00	0.00	0.00	0.00	0.00	0.00	0.00	0.00	0.00	0.00	0.00	0.00	0.00	0.00	0.00	0.00	0.00	0.00	0.00	0.00	0.00	0.00	0.00	0.00	0.00	0.00	0.00	0.00	0.00
Rb	104.91	103.03	100.88	103.55	102.55	89.76	90.35	84.34	88.67	103.24	110.47	107.97	107.14	105.40	136.49	99.27	112.06	97.14	91.24	108.81	81.32	96.97	109.26	84.51	89.33	95.60	109.64	113.85	90.03	99.94	100.88
Sr	129.43	122.02	98.03	109.36	132.80	106.47	104.87	131.13	102.12	125.16	174.98	112.08	142.00	169.33	87.51	123.86	104.43	135.98	117.04	139.28	102.67	118.25	124.18	120.45	107.30	79.89	108.10	120.64	99.25	123.84	100.45
Y	18.54	19.31	39.39	20.16	24.23	37.17	18.81	32.54	17.54	21.33	28.68	14.44	18.53	22.22	18.29	21.62	17.92	23.98	22.59	20.10	20.13	16.89	22.63	22.21	22.70	15.88	17.48	24.61	17.71	16.89	24.35
Zr	61.38	67.05	136.41	95.60	75.33	77.26	78.70	90.59	76.52	78.55	101.58	46.68	66.84	79.80	135.82	169.42	1352.74	117.40	81.80	68.68	72.37	63.39	491.37	93.87	65.27	57.57	82.57	86.47	111.45	85.16	65.62
Nb	14.48	16.53	17.71	26.10	13.60	10.40	11.78	76.03	14.16	15.63	19.08	7.59	8.68	16.65	14.63	16.26	16.71	24.18	19.53	24.54	15.53	11.96	11.83	12.14	11.28	10.80	13.71	16.30	11.35	6.90	17.77
Mo	0.24	0.27	0.38	0.33	0.44	0.42	0.35	0.60	0.25	0.72	0.39	0.85	0.37	0.06	0.79	0.34	0.47	0.40	0.62	0.39	0.58	0.85	0.99	0.46	0.30	0.49	0.32	0.49	0.68	0.44	0.52
Ag	0.17	0.12	2.55	0.30	0.18	0.22	0.32	0.41	0.17	0.17	0.20	0.67	0.34	0.16	4.81	0.18	1.04	0.16	0.18	0.17	0.17	0.34	0.69	0.42	0.38	0.00	0.25	0.26	0.21	0.26	0.04
Cd	0.57	1.17	4.00	0.30	0.75	0.51	1.15	2.76	1.09	0.52	0.73	3.86	1.27	5.00	3.90	0.38	2.17	0.35	0.57	0.72	1.09	1.99	1.35	2.08	0.67	2.26	1.74	0.99	0.68	1.02	0.00
In	0.05	0.06	0.16	0.02	0.07	0.05	0.08	0.19	0.06	0.06	0.06	0.09	0.07	0.00	0.18	0.04	0.10	0.05	0.06	0.09	0.04	0.12	0.10	0.08	0.05	0.06	0.08	0.07	0.08	0.07	0.02
Sn	17.25	2.59	1.35	2.91	3.22	3.22	1.98	6.63	2.45	2.12	3.05	1.14	11.47	3.88	6.41	2.92	3.71	3.50	7.73	10.50	2.53	2.87	8.64	3.31	6.37	1.55	2.53	2.88	4.81	1.62	2.66
Sb	0.96	0.54	0.79	0.41	0.56	0.39	0.35	0.66	0.24	0.89	0.48	0.43	0.80	0.48	0.41	0.39	0.75	0.43	0.52	0.54	0.44	0.63	1.23	0.71	0.35	0.34	0.45	0.49	0.76	0.52	1.66
Cs	5.24	6.03	6.30	4.83	5.20	4.48	4.45	4.15	5.21	5.17	6.63	3.23	4.83	5.80	6.06	6.17	5.63	5.54	4.52	5.11	5.85	4.14	5.20	5.16	4.65	4.84	5.64	6.44	3.61	4.04	4.46
Ba	355.55	448.46	421.39	355.83	466.44	294.44	371.21	328.79	347.93	346.07	456.90	305.88	418.82	475.56	417.75	336.71	406.61	404.23	315.84	368.77	308.49	316.53	483.41	350.64	356.47	311.83	388.15	501.26	371.79	361.51	378.74
La	23.46	29.51	31.52	25.30	22.01	29.53	19.33	22.80	21.61	23.60	32.88	16.15	21.31	21.30	20.50	28.52	21.06	26.79	20.61	21.37	23.49	19.99	23.04	23.39	22.17	22.00	23.11	30.11	25.41	19.06	26.86
Ce	53.03	60.80	55.41	59.27	44.44	58.39	43.16	46.12	46.96	55.32	77.83	37.55	49.12	41.21	45.87	64.03	43.01	52.21	46.38	46.46	47.24	41.73	49.36	51.86	52.44	50.76	44.02	62.22	59.45	41.13	56.62
Pr	5.90	7.31	8.33	6.49	5.65	7.75	4.58	5.80	5.55	6.44	9.25	4.18	5.69	5.26	4.91	7.39	5.35	6.76	5.85	5.37	6.02	4.97	5.52	5.93	6.14	5.62	5.77	7.75	6.23	4.70	7.27
Nd	19.59	24.80	32.88	22.00	20.20	28.32	15.58	22.05	18.88	23.67	34.95	15.33	20.56	20.30	17.89	25.10	22.32	23.67	24.69	20.04	20.18	19.15	21.37	22.50	20.30	20.88	21.60	29.14	21.73	16.17	26.48
Sm	4.16	4.28	8.33	4.70	4.30	5.14	3.18	5.27	3.82	4.82	7.58	2.26	4.41	3.34	3.35	5.14	5.15	5.29	4.35	3.89	4.26	4.19	5.06	4.94	4.33	3.12	4.15	6.29	4.23	3.48	4.72
Eu	1.05	1.02	1.53	1.07	1.00	1.42	0.85	1.41	0.90	1.11	1.75	0.61	1.15	0.79	1.05	1.14	1.23	1.11	1.09	0.94	0.94	1.13	1.21	1.23	1.03	0.66	1.01	1.41	0.89	1.06	1.13
Gd	3.95	3.51	8.81	5.03	4.06	4.82	3.24	5.74	3.61	3.92	5.72	2.02	4.02	3.84	3.19	4.47	5.95	4.60	4.20	3.71	3.98	3.89	4.69	5.29	3.71	3.21	3.79	5.36	3.64	3.13	4.41
Tb	0.66	0.53	1.14	0.82	0.64	0.94	0.54	0.81	0.57	0.66	0.88	0.37	0.63	0.56	0.44	0.64	0.81	0.71	0.63	0.55	0.60	0.79	0.58	0.74	0.61	0.46	0.56	0.81	0.55	0.55	0.65
Dy	4.03	2.95	6.35	4.47	3.75	5.50	3.25	4.83	3.22	3.76	4.99	1.78	3.70	2.82	2.52	3.78	3.60	4.31	3.74	3.06	3.40	4.09	3.85	4.17	3.69	1.98	3.33	4.49	2.98	2.88	4.21
Ho	0.72	0.59	1.03	0.69	0.74	1.26	0.66	1.00	0.66	0.76	1.03	0.29	0.69	0.70	0.60	0.77	0.65	0.85	0.77	0.66	0.66	0.85	0.78	0.81	0.74	0.60	0.67	0.88	0.61	0.57	0.79
Er	2.08	1.67	3.34	1.95	2.13	3.45	1.88	2.84	1.77	2.08	2.93	1.03	1.98	2.06	2.01	2.17	1.99	2.35	2.20	2.09	1.81	2.52	2.29	2.14	2.20	1.65	1.95	2.54	1.65	1.50	2.35
Tm	0.32	0.25	0.47	0.26	0.34	0.50	0.28	0.38	0.24	0.30	0.41	0.33	0.29	0.34	0.34	0.31	0.25	0.35	0.32	0.25	0.26	0.38	0.36	0.33	0.32	0.20	0.27	0.36	0.22	0.22	0.31
Yb	2.26	1.58	3.70	1.65	2.42	2.86	1.69	2.44	1.66	2.03	2.76	1.58	1.88	2.76	2.19	2.00	1.96	2.27	2.23	1.50	1.55	2.25	2.38	1.99	2.17	1.45	1.76	2.23	1.38	1.40	1.98
Lu	0.36	0.24	0.55	0.26	0.37	0.45	0.24	0.39	0.25	0.32	0.48	0.25	0.27	0.21	0.19	0.31	0.29	0.34	0.37	0.23	0.23	0.36	0.34	0.32	0.40	0.15	0.25	0.33	0.22	0.22	0.31
Hf	1.82	1.94	2.74	2.72	2.13	2.31	2.74	2.59	1.99	2.34	2.84	1.23	1.90	2.06	2.44	3.78	3.37	3.45	2.60	1.90	1.95	2.08	1.98	2.68	1.96	1.14	2.32	2.65	3.04	2.00	1.93
Ta	1.01	1.15	1.01	1.19	0.92	0.70	0.78	4.08	0.98	1.09	1.24	0.42	0.67	0.96	0.90	1.01	1.38	1.52	1.19	1.20	0.81	0.86	0.81	0.73	0.90	0.64	0.90	0.93	0.69	0.53	0.97
W	1.13	1.49	0.58	1.34	1.43	1.08	1.12	3.08	1.38	1.08	2.00	1.71	1.13	1.47	1.17	1.35	1.79	1.64	2.07	1.45	1.51	1.19	1.23	1.46	1.01	0.50	1.28	1.52	1.24	0.79	1.15
Au	0.00	0.00	0.00	0.00	0.00	0.00	0.00	0.00	0.00	0.00	0.00	0.00	0.00	0.00	0.00	0.00	0.00	0.00	0.00	0.00	0.00	0.00	0.00	0.00	0.00	0.00	0.00	0.00	0.00	0.00	0.00
Pb	28.42	27.03	22.39	22.28	25.00	21.60	18.22	22.43	23.66	29.67	23.90	22.50	21.34	22.61	27.68	19.91	33.67	17.06	20.28	20.50	21.18	26.74	38.44	57.76	19.84	20.73	18.14	23.49	38.39	19.96	21.46
Bi	0.03	0.44	0.14	0.20	0.22	0.19	0.16	0.39	0.14	0.33	0.23	0.23	0.41	0.26	0.40	0.02	0.36	0.21	0.20	0.16	0.32	0.57	0.18	0.12	0.20	0.23	0.52	0.26	0.05	0.17	0.05
Th	6.36	7.44	13.56	7.45	7.24	6.80	6.47	12.34	6.73	6.87	9.05	4.55	7.31	7.16	8.78	11.22	9.66	8.04	6.67	6.46	6.62	5.86	7.41	7.65	6.02	5.83	6.60	8.17	5.94	5.06	6.90
U	2.27	2.04	2.07	2.44	1.97	2.03	1.46	1.20	1.53	2.86	2.09	0.97	1.36	1.24	1.42	1.88	1.65	2.10	2.75	1.44	1.41	1.14	3.54	1.76	1.41	1.10	1.35	2.52	2.80	1.36	1.74

Be: city of Bruxelles

Table 4: (See color plate ••) Major, minor and trace elements composition of Brussels-made bricks
Tableau 4 : Composition en éléments majeurs, mineurs et traces des briques fabriquées à Bruxelles.

Chemical elements	Mean±SD (n = 31)	Range	Mean±SD A-type	Mean±SD B-type	Range A-type	Range B-type
$\%SiO_2$	77.94±2.28	73.15-82.13	77.05±2.2	79.21±1.65	73.15-80.70	76.64-82.13
$\%Al_2O_3$	10.3±1.13	8.42-12.29	10.61±1.07	9.92±1.08	8.84-12.12	8.42-12.29
$\%Fe_2O_3$	6.06±1.33	3.59-8.82	6.53±1.31	5.30±1.07	4.19-8.82	3.59-7.01
$\%K_2O$	2.11±0.3	1.46-2.8	2.08±0.30	2.15±0.30	1.46-2.61	1.68-2.80
%CaO	0.97±0.41	0.37-2.4	1.01±0.27	0.94±0.60	0.60-1.75	0.37-2.40
%MgO	0.93±0.14	0.63-1.22	0.98±0.12	0.86±0.12	0.81-1.22	0.63-1.06
$\%TiO_2$	0.73±0.32	0.29-2.23	0.73±0.15	0.73±0.52	0.43-0.98	0.29-2.23
$\%Na_2O$	0.68±0.15	0.33-0.98	0.66±0.12	0.70±0.19	0.47-0.85	0.33-0.98
$\%P_2O_5$	0.19±0.19	0.04-0.88	0.24±0.21	0.12±0.11	0.04-0.88	0.04-0.39
%MnO	0.09±0.04	0.04-0.26	0.10±0.05	0.07±0.01	0.26	0.05-0.09
SD: standard deviation						

Table 5: Chemical composition (mean, standard deviation and range of the major and minor elements) of the fired clay bricks of types A and B between the 14th and the 18th centuries.
Tableau 5 : Composition chimique (moyenne, écart-type, min-max des éléments majeurs et mineurs) des briques de types A et B entre le XIVe et le XVIIIe siècle.

In order to link the bulk composition of the brick matrix with its mineralogy (figure 6), we have adopted the graphical representation used in metamorphic petrology introduced by Eskola (1920) for representing phyllosilicate assemblages or the composition of the minerals occurring in siliciclastic rocks (Duchesne *et al.*, 2018). The figure 6 illustrates the position of several common minerals in siliciclastic rocks. Quartz is not represented but is the most common elemental constituent; the low content of Na_2O (<1%) and CaO (mean value <1%) is probably linked to the occurrence of

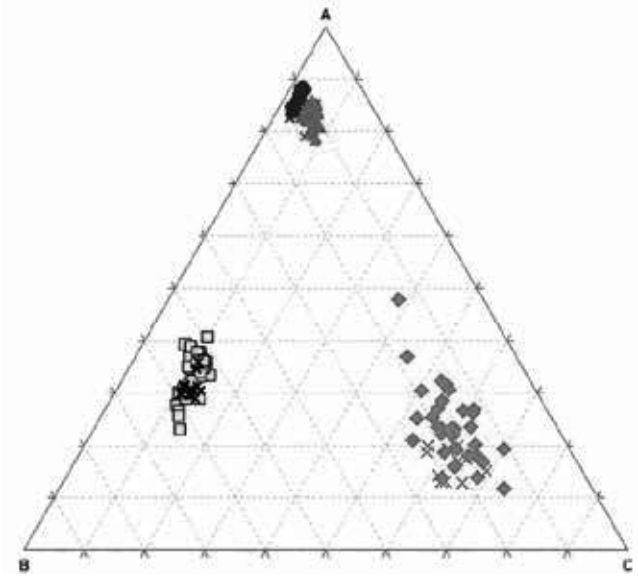

Figure 5: (See color plate ••) Ternary graph representing brick samples made from Brussels as a function of their main major chemical elemental compositions compared with loessic raw material. Bricks: Blue circles (A, B, C) = SiO_2 - Al_2O_3 - K_2O; red triangles: SiO_2 - Al_2O_3 - (Fe_{tot}+MgO); yellow squares: (Fe_{tot}+MgO) - Al_2O_3 - K_2O; green lozenges: CaO - Na_2O - K_2O; Loess: blue cross (A, B, C) = SiO_2 - Al_2O_3 - K_2O; red cross: SiO_2 - Al_2O_3 - (Fe_{tot}+MgO); black cross: (FeO+MgO) - Al_2O_3 - K_2O; green cross: CaO - Na_2O - K_2O.

Figure 5 : (Voir planche couleur ••) Graphique ternaire représentant la composition chimique en éléments majeurs des briques produites à Bruxelles comparées avec les matériaux lœssiques. Briques : cercles bleus (A, B, C) = SiO_2 - Al_2O_3 - K_2O; triangles rouges : SiO_2 - Al_2O_3 – (FeO+MgO); carrés jaunes : (FeO+MgO) - Al_2O_3 - K_2O; losanges verts : CaO - Na_2O - K_2O; Lœss : croix bleues (A, B, C) = SiO_2 - Al_2O_3 - K_2O; croix rouges : SiO_2 - Al_2O_3 - (FeO+MgO); croix noires : (FeO+MgO) - Al_2O_3 - K_2O; croix vertes : CaO - Na_2O - K_2O

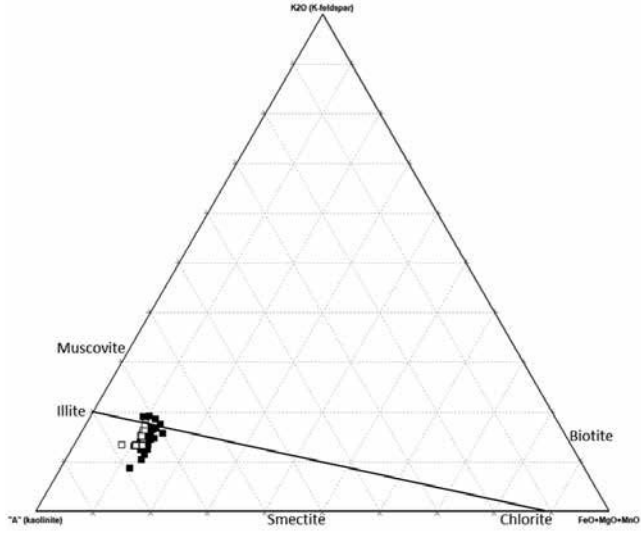

Figure 6: The AKF modified diagram. A represents %Al_2O_3 + %Fe_2O_3 - %(Na_2O + K_2O + CaO), K: %K_2O and the third pole (F) corresponds to %FeO + %MgO + %MnO. %FeO is estimated as 15% of %Fe_2O_3 total for all samples. Black squares: Brussels bricks, empty squares are loess.

Figure 6 : Le diagramme modifié AKF. A représente %Al_2O_3 + %Fe_2O_3 - %(Na_2O + K_2O + CaO), K : %K_2O tandis que le troisième pôle (F) correspond à la somme des %FeO + %MgO + %MnO. %FeO est estimé à 15% du %Fe_2O_3 total, calcul fait de manière identique pour chaque échantillon. Carrés noirs : briques de Bruxelles; carrés vides : læss.

plagioclases beside K-feldspars. Ca is partly distributed in apatite and, in rare cases, with a small proportion of carbonates. The position of the bricks in the diagram is indicative of a mixture of illite, kaolinite, smectite, and K-feldspars, with a small contribution of chlorites. Irregular mixed-layer illite/smectites probably occur in abundance. We can observe that loess samples are slightly richer in illitic compounds. Following Lindsey (1999, on-line, modifying Pettijohn *et al.*, 1972), the scattergram (figure 7), shows no difference between the type-A and the type-B for Al_2O_3/SiO_2, while a minor difference can be observed for (Fe_2O_3+MgO)/(Na_2O+K_2O). Some scattergrams (figures 8 & 9) show the relationship between certain chemical elements and the mineralogy and nature of raw materials. For the same K-content, type-A bricks are richer in alumina compared to type-B and loess, likely because of partial K-leaching from the illitic components and/or weathering of K-feldspars during pedogenic processes (gleysols). These two last figures show that loess sediments have a chemical composition closer to the brick of type-B. The figure 9 shows enrichment in Al and Mg in type-A bricks, indicative of a probable gleysol illuviation.

REE concentrations in soils vary according to parent material properties, history and weathering state of the soil, organic matter content, and clay minerals… The distribution of chondrite normalized Rare Earth Elements (REEs) (not illustrated in this paper) does not allow differentiation between type-A and type-B bricks as they have similar profiles and show overlap indicating that the gleyification process has no influence on the REE concentrations (no depletion or enrichment). The profiles are characterized by a clear negative Eu anomaly and slight positive Ce anomaly. REE patterns of loess samples are very similar to those acquired on bricks. These similarities can be explained by a predominance of loess in the raw material for making bricks. Rare detrital grains of monazite (REE-rich phosphate mineral) were observed in thin-sections of bricks and analysed by EDS.

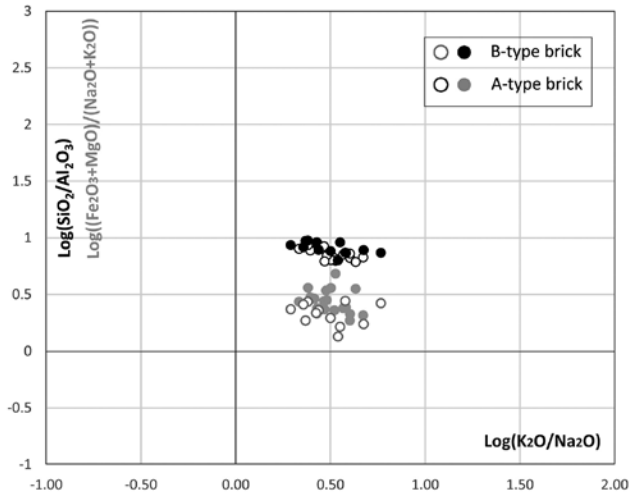

Figure 7: Combined scattergrams showing brick composition (after Lindsey, 1999, on-line).
Figure 7 : Diagrammes combinés montrant la composition des briques (d'après Lindsey, 1999, on-line).

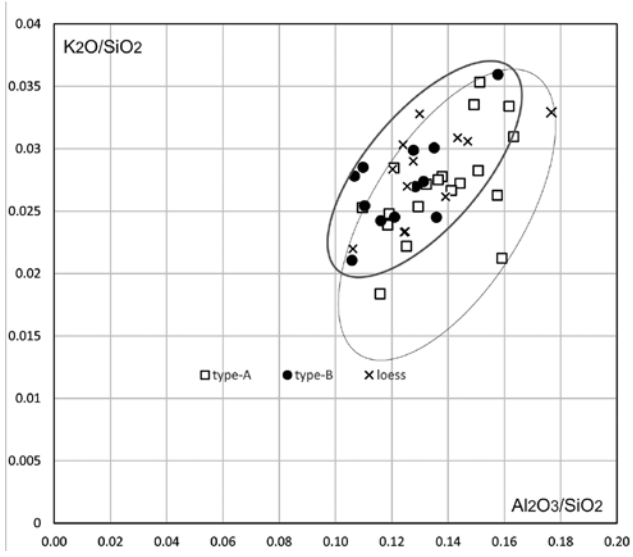

Figure 8: Scattergram showing the composition of bricks and the relation between Al and K normalized to Si.
Figure 8 : Diagramme montrant la composition des briques et la relation entre Al et K normalisés par rapport à Si.

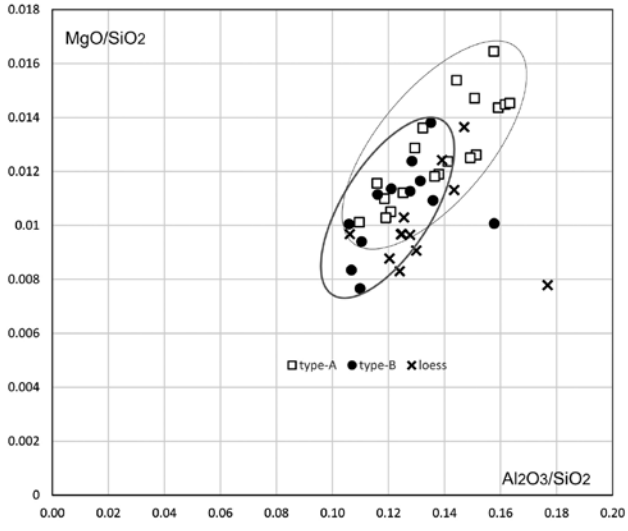

Figure 9: Scattergram showing the composition of bricks and the relation between Al and Mg normalized to Si.
Figure 9 : Diagramme montrant la composition des briques et la relation entre Al et Mg normalisés par rapport à Si.

Geochemical data were statistically treated to identify groups of chemically similar bricks. These groups are interpreted as made from the same raw materials and therefore presumably in the same place, although not necessarily at the same time (Nunes *et al.*, 2013). Alteration (heating and firing) and contamination (lime mortar), perhaps due to post-depositional processes, normally modify the original composition of ceramics (Buxeda & Garrigós, 1999).

A dendrogram (figure 10) provides a straightforward method of displaying cluster similarity semi-quantitatively, but the two types of bricks and loess are not clearly differentiable, indicating a strong chemical resemblance. Type-A bricks are slightly richer in iron and phyllosilicates (table 5) due to the influence of pedogenic processes in the raw material deposits. However, the data do not allow us to discriminate between different brickyards, nor isolate the production of Uccle and Auderghem. In order to understand the behaviour of chemical elements an R-mode principal component analysis (PCA) (figure 11) was applied to the bricks. The first six factors represent 70% of the total variance in the brick data. The first factor (32%) is negatively correlated with Si, K and Na and positively loaded with Rare Earth Elements (REEs) and a large group of other elements (Mg, Fe, Ba, Ti, Ca). The first elements represent detrital quartz and feldspars (K-feldspars and plagioclases) relative to other detrital minerals. The second factor is difficult to decipher and seems to oppose plagioclase minerals with K-feldspar and chlorites, while the third factor opposes clays minerals with quartz and resistant minerals. The three other factors are difficult to interpret and contain only minor and trace elements.

x-ray Diffraction

Mineralogy and firing temperature have a direct influence on the porosity of bricks and their properties (Cultrone *et al.*, 2004). As expected and observed by optical petrogra-

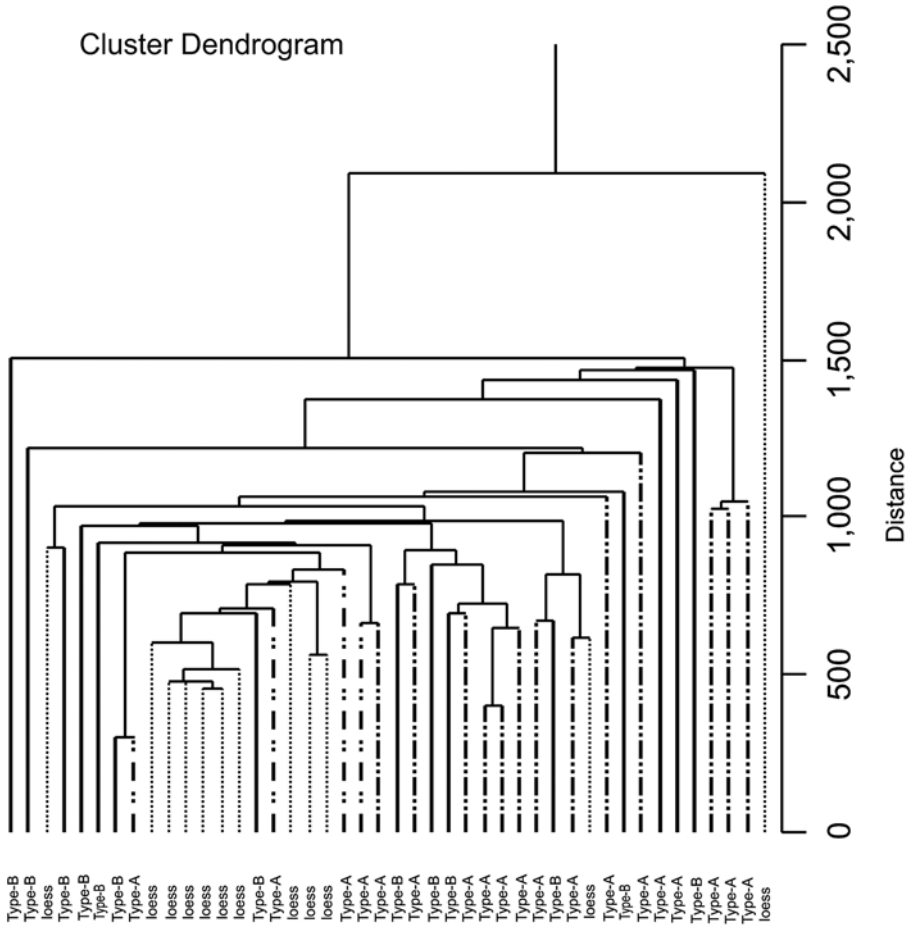

Figure 10: Schematic representation of a hierarchical cluster analysis (HCA) of multidimensional geochemical data of the bricks and compared with loess samples.

Figure 10 : Classification hiérarchique ascendante (HCA) des données géochimiques obtenues sur les briques et comparées avec les échantillons de læss.

phy, quartz is the major constituent (table 6) of the bricks. Feldspars (K-feldspar and/or plagioclases) are present in every sample. Detrital feldspars are identified in thin section in very low concentrations; their higher proportions in fired clays are due to neoformation of K-feldspar from illitic clay minerals. The most significant mineralogical changes during firing are the dehydroxylation of kaolinite around 490°C (with formation of metakaolinite as a sintering agent), the disappearance of clay minerals above 800°C and the breakdown of micas starting at 900°C, as well as the occurrence of a significant amount neoformed K-feldspars, plagioclase and hematite. Traces of clay minerals and minor amounts of muscovite ("10 Å" peak) indicate bricks fired below 900°C. A "10 Å" peak is occasionally observed on the diffractograms, grouping mica flakes (mainly muscovite), illite and glauconite, but also other clay minerals such as smectites and irregular illite-smectite mixed layers, which are collapsed at 10 Å over 300°C. They are grouped together because X-ray diffraction on powdered samples does not allow discerning between the individual spectra. Most bricks contain a small amount of hematite, on the order of a few percent or below the detection limit. The XRD background profile is flat and lacks the broad hump usually present at 2θ = 9.05-9.38 in thermally treated clays (Pavía, 2006). This is indicative of the absence of amorphous compounds. Small amounts of calcite in some bricks represent secondary calcite, precipitated from lime mortar in fractures or the connected pore network. The non-calcareous matrix does not develop distinctive Ca-bearing silicates. High temperature (>1050-1100°C) phases as mullite or cristobalite are not present, but pyroxenes and olivine occur in samples PS-45 and 8 respectively, indicative of a Fe-rich silty matrix and high temperature. The temperature range of the bricks is between 700°C and 1100°C and the brick colour seems to be temperature dependant. At 700 to 800°C, the clay displays an orange-cadmium to light red colour, whereas above 900°C, it turns to a deeper red colour, probably due to an increase in the amount of neoformed hematite (Pavía, 2006).

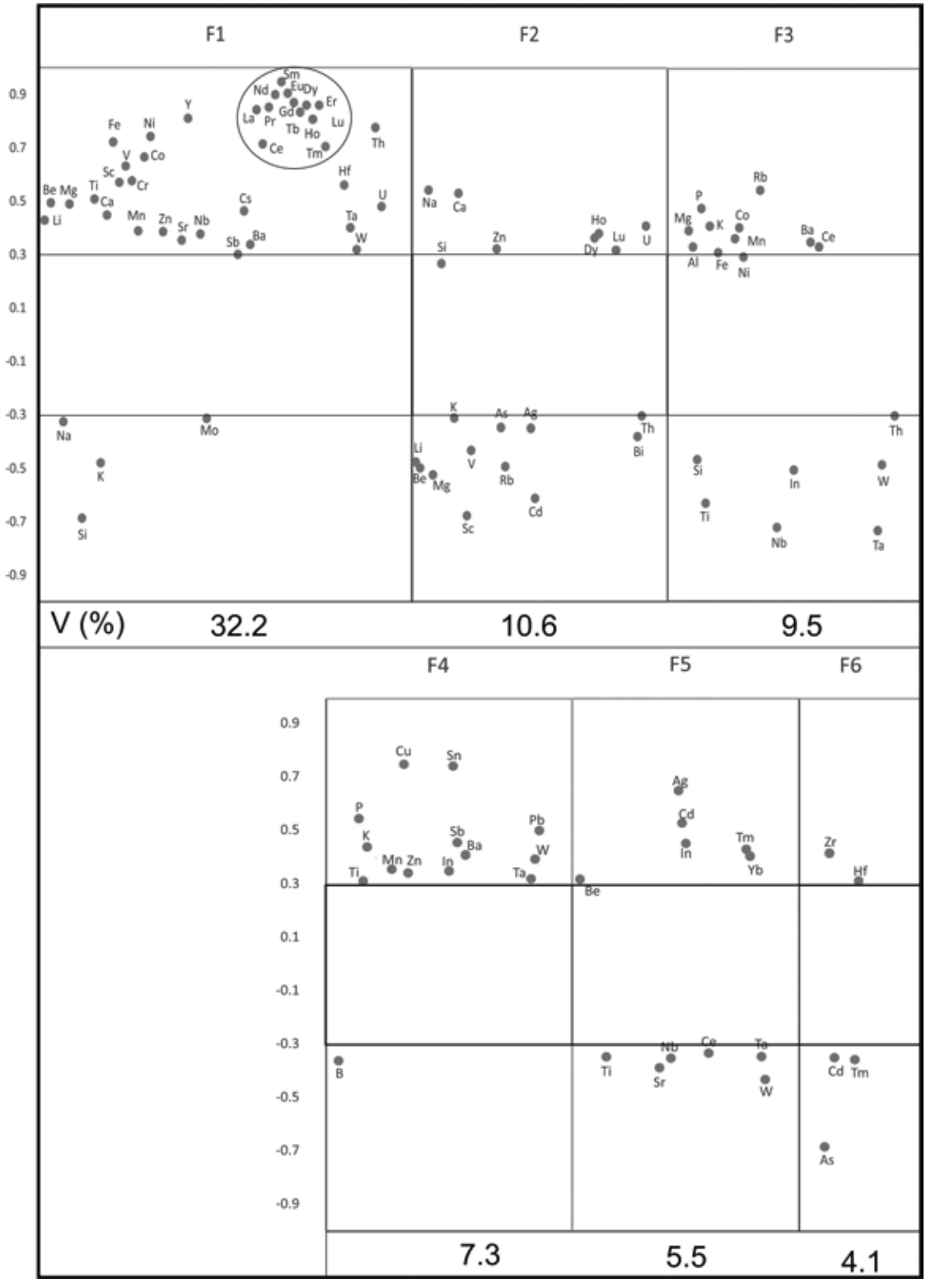

Figure 11: Graphical representation of the factor loading of the six principal components calculated for the bricks. V (%) is the proportion of total variance expressed by the components.
Figure 11 : Graphe construit sur base de l'analyse en composantes principales sur base des 6 facteurs principaux représentant 69% de la variance totale (V%).

	% 10Å complex	% Quartz	% K-feldspars	% Plagioclases	% Hematite	% Pyroxene	% Calcite	% Smectite	% Gypsum	% Olivine
PS-5		83.85	14.31		1.84					
PS-8		74.72	8.59	7	4.66					5.03
PS-14		72.31	25.17		2.53					
PS-15		73.98	24.78		1.24					
PS-17		76.49	21.76		1.75					
PS-18		70.01	27.99		2					
PS-19		77.17	20.87		1.96					
PS-23	10.57	79.24		10.19						
PS-24		72.98	24.39		2.62					
PS-25	8.27	81.69		10.04						
PS-26	8.26	67.2	23.94		0.61					
PS-27		95.46		2.52	2.02					
PS-28		69.59	29.32		1.08					
PS-29		72.94	20.5	5.73	0.84					
PS-30	2.95	69.2	22.7	4.39	0.75					
PS-33		69.56	28.61		1.83					
PS-34		70.07	29.27		0.66					
PS-35		70.01	16.36	13.28	0.35					
PS-41	3.47	74.9	21.62							
PS-42		71.31	25.88		2.82					
PS-44	3.92	66.05	21.85	7.23	0.95					
PS-45	7.71	69.8	11.13	6.01				5.34		
PS-47		65.68	33.52				0.81			
PS-48	6.99	75.62	14.4	2.99						
PS-50		79.96	11.06	5.64	3.34					
PS-51		68.82	29.7		1.48					
PS-52		74.79	18.1	5.52	1.58					
PS-53		88.2		10.63			1.17			
PS-67		44.7	26.2	12.92	0	12.76	3.02		0.4	

Table 6: Mineralogical composition (% of the crystalline phases) of the silty matrix of the bricks determined by X-ray diffraction.
Tableau 6 : Composition minéralogique (% des phases cristallines) de la matrice silteuse des briques déterminée par diffraction des rayons X.

Scanning electron microscope and energy dispersive spectroscopy

Using an analytical scanning electron microscope with X-ray dispersive spectroscopy, data were obtained on the composition of the clayey matrix and non-clay minerals and the degree of vitrification and firing temperatures. These techniques were applied to polished sections of both of type-A and type-B bricks, showing different states of hardness, but also to moulding sands and lime mortar (not presented in this paper). Some results are illustrated on plate 1.

At low firing temperature, prior to the onset of vitrification, the matrix consists of detrital quartz (dominant, inequant to equant sub-rounded grains), small amounts of K, Na-Ca and K-Na-Ca feldspar particles, mica flakes (muscovite, biotite), Fe-chlorite flakes, and some glauconite grains, all in a fine textured microcrystalline matrix without vitrification. The clay matrix is mainly composed of Si, Al and to a lesser extent Fe, K, Ca, Na and Ti. In some cases, phosphorus is present even though no calcium phosphate is observable. In high-fired bricks, an amorphous matrix appears at the beginning of vitrification process, where the clay matrix breaks up to form a fine network of relict-clay (rich in neoformed feldspars) interconnecting the detrital quartz grains. High-fired bricks can easily be cut and polished, while low-fired bricks are very brittle and cannot be polished, even using a fine grained silicon carbide.

All bricks are porous. Unconnected pores occur as mesopores to megapores as seen in thin sections. Microporosity is mainly visible in lower fired bricks, but progressively disappears during the vitrification process, replaced by macroscopic vesicles and microscopic bloating pores accompanied by a change of colour, from red to grey-black. Only areas of the matrix that were overheated show vitrification under the SEM. The biggest pores are observed in iron glaebules as ring voids or radial voids as a result of the release of water

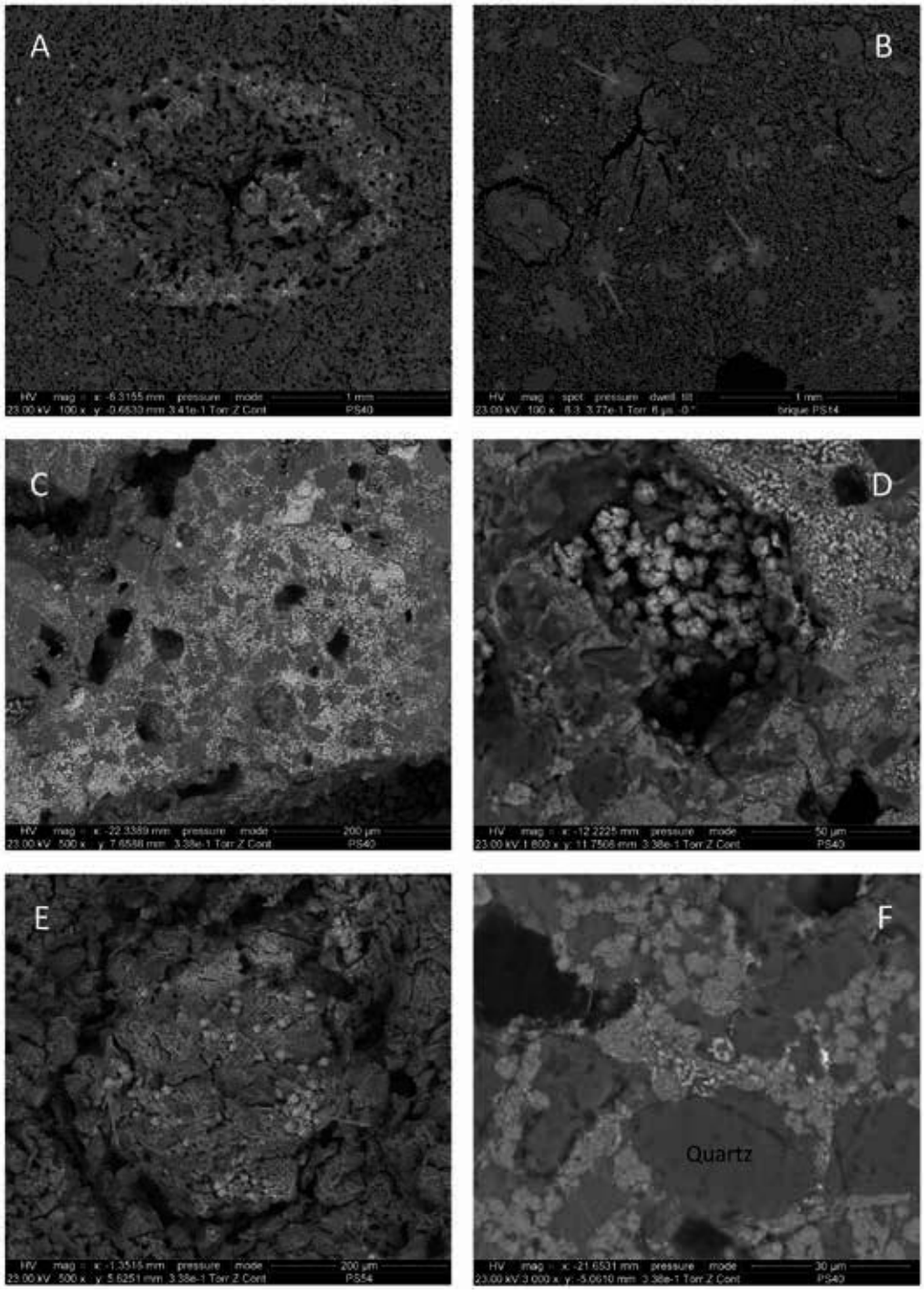

Plate 1: A) PS-40: gley patch rich in iron oxide (lighter grains). The iron rich concretion is rounded by a ring void. The voids size is larger in the concretion than in the brick matrix; B) PS-14: calcium rich concretion (red arrows) in brick matrix. The quartz grains are cemented with calcite that contain aluminosilicate particles (phyllosilicates); C) PS-40: iron oxide-rich zone in gley patch. Iron oxide is present as micrometric rounded crystals; D) PS-40: aggregates of magnetite octahedral crystals; E) PS-54: iron oxide rich concretion with framboids (red arrows), probably pseudomorphose of pyrite in iron oxide; F) PS-40: gley patch. Quartz grains are cemented by the combination of two kinds of oxides. A (Mn,Fe) oxide present as "cores" grains (red arrows) surrounded by a (Fe,Mn) oxide (blue arrows).

Planche 1: A) PS-40 : tache de gley riche en oxydes de fer (grains de tonalités claires). Cette concrétion riche en fer est entourée par un pore circulaire. La taille des pores est plus grande dans la concrétion que dans la matrice de la brique ; B) PS-14 : concrétion riche en calcium (flèches rouges). Les grains de quartz sont cimentés par de la calcite qui renferme des particules d'aluminosilicates (phyllosilicates) ; C) PS-40 : zone riche en oxydes de fer à l'intérieur d'une tache de gley. L'oxyde de fer est présent sous la forme de cristaux micrométriques arrondis ; D) PS-40 : agrégats de cristaux octaédriques de magnétite; E) PS-54 : concrétion riche en oxydes de fer avec des framboïdes (flèches rouges), probablement de pseudomorphose de pyrite en oxydes de fer ; F) PS-40 : tache de gley. Les grains de quartz sont cimentés par la combinaison de deux types d'oxydes. Un cœur d'oxyde (Mn,Fe) (flèches rouges) est entouré par un autre oxyde (Fe,Mn) (flèches bleues).

during drying phases (dry season in pedogenic profiles and crude brick drying), accentuated by dehydroxylation in the phyllosilicates (Elert *et al.*, 2003) and the transformation of iron hydroxides to iron oxides during the firing. Iron is widely present in bricks under various forms (Fe-rich minerals, matrix impregnation, glaebules or patches…). Red spots are made of impure hematite (xenomorphic to pseudohexagonal plates) while dark brown to grey-black spots differ. Under the SEM, octahedral minute crystals were observed in the concentric or radial pores crosscutting brown-blackish spots (type-A bricks) (plate 1) attributed to magnetite. The presence of a small amount of manganese (up to 10%) shows that the mineral neoformed during firing, has a spinel structure and a composition between magnetite (Fe_3O_4) and jacobsite ($MnFe_2O_4$). In some glaebules, rounded detrital quartz grains are surrounded and/or cemented by (Mn,Fe)-oxides showing a zonation in the Mn:Fe ratio. These features require analysis by electronic microprobe for determination of the proportions and oxidation state of the coupled iron-manganese. As a consequence, the Fe glaebules must be called Fe-Mn glaebules and the zonation is directly related to the successive (seasonal) precipitations of these two elements during pedogenic processes affecting gleysols. Pavía (2006) also observed micrometric octahedral crystals of spinel (magnetite) and pseudo-hexagonal crystals of hematite in a cinder inclusion, though the general morphology is similar to pedogenic iron-rich patches. However, Pavía does not give arguments for the presence of cinders in Irish bricks from Rathfarham Castle. He explains that these types of inclusions are the remains of burned organic fuel.

Heavy detrital minerals such as ilmenite, leucoxenes (with large variation of the Ti:Fe ratio), rutile, zircon, monazite and secondary minerals such as barite, calcium carbonate and calcium sulphate are accessory phases easily identified by secondary and backscattered electron imaging. Additionally some grains are very rich in Ca and to a lesser extent in Fe, Si, O and sometimes Al. This/these calcium silicate(s) represent high-temperature calcium-aluminium silicates like hedenbergite ($CaFeSi_2O_6$), a ferro-hornblende [$\square Ca_2(Fe_4^{2+}Al)(Si_7Al)O_{22}(OH)_2$], or other minerals. We rarely observe quartz grains cemented by primary calcite, these are characteristic of minute rock fragments, faecal pellets and loess puppet fragments. Moulding sands observed under the SEM confirm prior observations. The microstructure of the forams and other microfossils shows the precipitation of secondary gypsum in the stalls, and patches of biogenic phosphate.

Magnetic Susceptibility (MS)

Archaeomagnetic studies applied to archaeological fired clay (tiles, bricks, ceramics and kiln walls) are conducted mainly to date the fired structures and furnish new information on production (Hus, 2003; Hus *et al.*, 2002, 2003; Lanos, 1987, 1999), while data of the average magnetic susceptibility (K_{av}) is rarely published in the literature. High magnetic susceptibility values are due to variations in the concentration and grain size of the magnetic minerals in these sediments (Maher & Thompson, 1995) used to produce bricks. In fired products, MS is also influenced by the C-content of the raw material, the heating atmosphere and the firing temperature (Hus, 2003; Hus *et al.*, 2002, 2003) to neoform magnetite instead of haematite. Measurements of the bricks fall in a large range between 0.15×10^{-6} and 14.7×10^{-6} m^3/Kg (mean: 2.6×10^{-6} m^3/Kg, StDev: 3.99×10^{-6} m^3/Kg). MS values are neither correlated to the iron content of the matrix nor the age of the brick. The highest values ($>10^{-5}$ m^3/Kg) are directly linked to the dark brown and grey black pedogenic glaebules rich in magnetite octahedrons and magnetite/jacobsite concretions as observed with the SEM. Magnetite is ferromagnetic, while jacobsite is diamagnetic but for materials that show ferromagnetism, the diamagnetic contribution becomes negligible. Note that magnetite was identified by XRD only in the sample with the highest measured MS value, while for the other bricks, the magnetite content is below the detection limit. The firing atmosphere is the predominant factor that controls susceptibility enhancement in bricks.

6. Sourcing of the raw material

Our results suggest that the two types of Brussels bricks were made with two locally gathered "clays". Both macroscopic and microscopic observations show that the raw materials were derived from gleysols (type-A) and fluvisols (type-B) with gleyic fluvisols in between. They differ by whether characteristic pedogenic processes, colour mottling, segregation processes i.e. the redistribution of iron, or the intensity of destratification, have occurred or not. Although bricks made from gleysols are globally richer in Fe and Mn, they have the same mineral and chemical matrix composition. Raw materials for both are found in the same environmental conditions but represent different layers.

A fluvisol in the FAO World Reference Base for Soil Resources is defined as a genetically young soil in alluvial deposits and occur in the Senne alluvial plains. Under natural conditions periodic flooding was fairly common,

and parent material was derived from the Senne sedimentary basin. Sediments deposited in the Senne alluvial plain consist of sediments reworked from adjacent highlands made of a thick cover of Quaternary loess and Tertiary loose sands and clays deposited during the Pleistocene and Holocene. During inundation, silt drops from the retreating floodwater and, trapped by vegetation, tends to build up and level the floodplain surface. The Senne floodplain deposits show vertical size-graded stratification (sorting). These soils have a clear evidence of stratification and soil horizons are weakly developed. Sedimentary features (small-scale stratification) from the original utilized clay deposits are visible in type-B bricks because the paste was not blended before forming (poorly/non-mixed fabric). Remnant stratification is sometimes shown by a very thin layer of well sorted medium-grained sand (quartz and flint) indicating that the sand was not added as temper to the clay paste.

Gley soils are grouped under gleysols which occur in alluvial floodplains. They exhibit a greenish-blue-grey soil colour due to anoxic wetland conditions. Anaerobic conditions lead to the reduction of iron from its ferric state to its ferrous state (gleying), which is soluble in soil water and moves in the profile. Where the water table fluctuates, ferrous iron dissolved in the groundwater can be reoxidized and is deposited when it meets oxygenated areas of the soil or along root channels. The result is reddish mottles, nodules and iron pans within an otherwise blue-grey matrix. This redoxomorphic colour pattern is typical of hydromorphic soils. Additionally, petrographic observations on bricks made from gleysols show infiltrated, illuviated clays occurring in cutans along bounding block peds (clay skins) around framework grains, dispersed throughout the sediment or along permeable channels. Clay minerals and iron (+ Mn) together form argilans or ferri(+Mn)-argilans respectively. Framework grains of quartz (or micas flakes) with coatings of iron oxide, iron-rich haloes, incipient iron oxide nodules (with diffuse boundaries), rounded shape nodules (with distinct boundaries), concentric-banded nodules, iron-concretions around "disappeared" former (decayed or burned) root tubes and radiated cracks nodules, ferri-argilans, and (partial) destratification are frequently observed in type-A bricks. Nodules vary in size from 0.5-1 cm across. Pedogenic slickensided surfaces were not observed, due to the low content of swelling clays and an unfavourable climate without extremes of wetting and drying (Bridge, 2003). Gley soils may be sticky and hard to work, especially where the gleying is caused by surface water held on a slowly permeable layer. Good drainage is required for cultivating these soils, but these soils are good raw material for the production of architectural terracotta.

The presence, even relictual (type-A), of stratification planes demonstrates the absence of preparation of the raw loam. Although no organic fuel had been added to the paste for the same reason, it is possible that finely disseminated organic matter and roots occurred in the raw material and contributed as combustible matter. This natural organic matter can be responsible for the incomplete oxidation of the iron in some places and the synthesis of iron-rich spinel (series magnetite-jacobsite).

7. Conclusions and perspectives

Two types of bricks were produced in Brussels with alluvial loams gathered in the alluvial plain of the Senne valley. The oldest bricks were made with gleysols while the more recent ones used raw material from fluvisols, probably coming from deeper layers. Mining of deeper layers may be due to a better anthropic drainage of the alluvial plain leading to the progressive transformation of a humid plain to a more cultivable plain. Tertiary sands from the Lede Formation were extracted in the valley sides to produce moulding sands. All brickyards used raw materials coming from the same sedimentary environment, and consequently, it is impossible to identify the exact brickyard where any given brick was made. But the bricks made in Brussels have a particular signature due to the reworking of Quaternary loess deposits mixed with small amounts of Palaeozoic, Cretaceous and Tertiary sediments. This first archaeometric study of brick production in Belgium can be applied to other Belgian cities and production areas in Belgium and in the Netherlands to gain a better understanding of the circulation of these products.

Engineers are concerned with mechanical behavior, water absorption and permeability, and durability. However, physical characteristics such as bulk density, water absorption, and characteristic strength are totally unknown for Belgian historical bricks, opening an interesting field of research. It could be interesting to study the microstructure and current mechanical properties of historical bricks from Brussels, both for facades and inner walls, to know if differences can be related to various provenances. These qualities of bricks are important for controlling moisture (moisture repellent, buffering capacities), thermal inertia properties, acoustic comfort, fire resistance (and no damaging flue gas emissions), and longevity.

Subsequent papers will be devoted to the characterization and provenance of a) bricks imported to Brussels after its bombing by the troops of Louis XIV, b) the lime-mortar between the 14th and the 18th centuries and c) the use of slate wedges in the masonry.

Remerciements

The authors warmly thank many colleagues for answering their requests and for generously sending documentation, information, material for comparison, and analytical results. We would like to mention in particular Britt Claes (archaeologist, Museum of Art and History, Belgium), Paulo Charruadas (Historian and archaeologist, Université libre de Bruxelles, Belgium), Lou Cognard (conservator, Museum of Art and History, Belgium), Ann Degraeve (archaeologist, Monuments and Sites Directorate of the Brussels Regional Public Services, Belgium), Stéphane Demeter (historian, Monuments and Sites Directorate of the Brussels Regional Public Services, Belgium), Marianne Dingemans, Jeroen Krijnen (archaeologist, Gemeenten Zutphen, Netherlands), Sylvianne Modrie (archaeologist, Monuments and Sites Directorate of the Brussels Regional Public Services, Belgium), Edwijn Orsel (Archaeologist, Erfgoed Leiden, Netherlands), Jef Pinceel (conservator, Museum of Art and History, Belgium), Gabri van Tussenbroeck (archaeologist, Universiteit van Amsterdam, Netherlands), Bram Vannieuxenhuyze (historian, University of Amsterdam, Netherlands) and Michel de Waha (Historian and archaeologist, Université libre de Bruxelles, Belgium), Laure Dussubieux (Field Museum, United States) and Rebecca Deeb (University of Illinois at Chicago, United States). We thank anonymous reviewers.

References

Arntz, W.J.A., 1971. De middeleeuwse baksteen. *Bulletin van de Koninklijke Nederlandse Oudheidkundige Bond*, 70 (4): 98-103.

Balestracci, D., 2000. Produzione e uso del mattone a Siena nel Medioevo. *In* P. Boucheron, H. Broise, Y. Thébert (eds.). *La brique antique et médiévale. Production et commercialisation d'un matériau.* Ecole française de Rome, Rome, 417-428 et 443-445.

Blain, S., 2011. Les terres cuites architecturales des églises du haut Moyen Age dans le nord-ouest de la France et le sud-est de l'Angleterre. Application de la datation par luminescence à l'archéologie du bâti. *British archaeological report – BAR International Series 2189*, Oxford.

Blanquart, P., 2001. Preventieve opgravingen op de site van de voormalig warenhuis Esders aan het Sint-Katelijneplein. *In* P. Blanquart, S. Demeter, A. De Poorter, C. Massart, S. Modrie, I. Nachtergael, M. Siebrand (eds). *Autour de la première enceinte*. Collection : *Archéologie à Bruxelles*, 4: 29-53.

Bridge, J.S., 2003. *Rivers and floodplains: Forms, processes, and sedimentary record*. Blackwell publishing, 504p.

Buffel, P., Matthijs, J., 2002. Geological map of Bruxelles-Nivelles n°31-39, 1/50.000-scale map and *Brussel-Nijvel, Toelichtingen bij de geologische kaart van België* published by the Flemish Region and carried out jointly by the Geological Survey of Belgium and the Ministry of the Flemish Community.

Buxeda, I., Garrigós, J., 1999. Alteration and contamination of archaeological ceramics: the perturbation problem. *Journal of Archaeological Science*, 26 (3): 295-313.

Cabuy, Y., Degré, S., 1993. Intervention place Saint-Gery. Structures médiévales et post-médiévales. *Bulletin du Crédit Communal*, 182: 16.

Camerman, C., 1955. Le sous-sol de Bruxelles et ses anciennes carrières souterraines. *Annales des Travaux Publics et de la Reconstruction*, 2: 5-28.

Castro, F., 1999. Statistical and analytical procedure for the estimation of the provenance of archaeological ceramics. *Proceedings of the 4*th *European congress on old ceramics*, Andorra, 52-58.

Coomans, T., van Royen, H., 2008. *Medieval Brick Architecture in Flanders and Northern Europe: the question of the Cistercian origin*. Abdijmuseum "Ten Duinen 1138", Koksijde & Academia Press publishers, 330p.

Culot, M., Hennaut, E., Demanet, M., Mierop, C., 1992. *Le bombardement de Bruxelles par Louis XIV et la reconstruction qui s'en suivit 1695-1700*. AAM Editions Paris - Bruxelles, 300p.

Cultrone, G., Sebastián, E., Elert, K., De La Torre, M.J., Cazalla, O., Rodriguez-Navarro, C., 2004. Influence of mineralogy and firing temperature on the porosity of bricks. *Journal of the European Ceramic Society*, 24 (3): 547-564.

Danckaert, L., 1989. *Bruxelles. Cinq Siècles de cartographie*. Lannoo Uitgeverij, Tielt-Knokke, 144p.

Debonne, V., 2008. Bouwen met baksteen in het Kortrijkse en het Oudenaardse tijdens de middeleeuwen. *In* T. Coomans, H. van Royen (eds). *Medieval Brick Architecture in Flanders and Northern Europe: the question of the Cistercian origin*. Abdijmuseum "Ten Duinen 1138", Koksijde & Academia Press publishers, 185-202.

De Maeyer, Ph., Serruys, E., Meire, E., Lapon, L., 2012. *A concise geography of Belgium*. National Committee of Geography of Belgium Eds, IGU, 46p.

Demeter, S., Sosnowska, P., 2007. Sur les traces des comtes de Mansfeld à Bruxelles, les vestiges archéologiques découverts dans l'hôtel de Merode. *In* J.-L. Mousset, K. De Jonge (eds). *Un prince de la Renaissance. Pierre-Ernest de Mansfeld (1517-1604), II, Essais et catalogue*. Musée national d'histoire et d'art, Luxembourg, 49-54.

De Poorter, A., 1995. *Au quartier des Riches-Claires : de la Priemspoort au couvent*. Co-edited by the Musées royaux d'Art et d'Histoire and the Fabrique d'église de Notre-Dame des Riches-Claires. Collection : *Archéologie à Bruxelles*, 1, 216p.

Devleeschouwer, X., Pouriel, F., 2005/2006. The subsurface geology of Brussels, Belgium, is modelled with 3D GIS. From http://www.esri.com/news/arcnews/winter0506articles/subsurface-geology.html, consulted 04/2018.

De Waha, M., De Poorter, A., 1993. Een historisch symbool te Brussel, de Hallepoort. Resultaten van de eerste archeologische opgravingen in de Hoofdstad. *Overdruk uit het Tijdschrift van het Gemeentekrediet*, 182: 30-36.

Dewilde, M., 2008. Bouwen met baksteen in middeleeuws Ieper. *In* T. Coomans, H. van Royen (eds). *Medieval Brick Architecture in Flanders and Northern Europe: the question of the Cistercian origin.* Abdijmuseum "Ten Duinen 1138", Koksijde & Academia Press publishers, 233-241.

Diekmann, A., 1997. *Artisanat médiéval et habitat urbain*, *rue d'Une Personne et place de la Vieille-Halle-aux-Blés.* Collection : *Archéologie à Bruxelles*, 3, 158p.

Dikstein-Bernard, C., 2007. La construction de l'Aula Magna au palais du Coudenberg. Histoire du chantier (1452-1461). *Annales de la Société Royale d'Archéologie de Bruxelles*, 68: 37-64.

Dreesen, R., Dusar, M., Dopere, F., 2003. *Atlas natuursteen in Limburgse monumenten : geologie, beschrijving, herkomst en gebruik*. Published by Provincie Limburg, Hasselt, 294p.

Dreesen, R., Dusar, M., 2004. Historical building stones in the province of Limburg (NE Belgium): Role of petrography in provenance and durability assessment. *Materials Characterization*, 53 (2-4): 273-287.

Druc, I.C., Inokuchi, K., Dussubieux, L., 2017. LA-ICP-MS and petrography to assess ceramic interaction networks and production patterns in Kuntur Wasi, Peru. *Journal of Archaeological Science: Reports*, 12: 151-160.

Duchesne, J.-C., Meus, Ph., Boulvain, F., 2018 (available online since 14/11/2017). Geochemistry of Lower Devonian terrigenous sedimentary rocks from the Belgian Ardenne: source proxy and paleogeographic reconstruction. *Sedimentary Geology*.

Duhamel du Monceau, H.-L., Fourcroy de Ramecourt, C.-R., Gallon, J.-G., 1763. *L'Art du tuilier et du briquetier*. Paris, 67p.

Dunham, A.C., 1992. Developments in industrial mineralogy: I. The mineralogy of brick-making. *Proceedings of the Yorkshire Geological Society*, 49 (2): 95-104.

Elert, K., Cultrone, G., Navarro, C.R, Pardo, E.S., 2003. Durability of bricks used in the conservation of historic buildings—influence of composition and microstructure. *Journal of Cultural Heritage*, 4 (2): 91-99.

Eskola, P., 1920. The mineral facies of rocks. *Norwegian Journal of Geology* (*Norsk Geologisk Tidsskrift)*, 6: 143-194.

Firman, R.J., 1994. The colour of brick in historical brickwork. *British Brick Society Information*, 61: 3-9.

Firman, R.J., Firman, P.E., 1967. A geological approach to the study of medieval bricks. *The Mercian Geologist*, 2 (3): 299-318.

Fourny, M., 1994a. Les fouilles de la cave du n°24, rue au Beurre. *Annales de la Société royale d'Archéologie de Bruxelles*, 59: 57-65.

Fourny, M., 1994b. L'église Notre-Dame du Finistère. 2. La fouille. *Annales de la Société royale d'Archéologie de Bruxelles*, 59: 234-252.

Gialanella, S., Girardi, F., Ischia, G., Lonardelli, I., Mattarelli, M., Montagna, M., 2010. On the goethite to hematite phase transformation. *Journal of Thermal Analysis and Calorimetry*, 102 (3): 867–873.

Glascock, M.D., Anderson, M.P., 1993. Geological Reference Materials for Standardization and Quality Assurance of Instrumental Neutron Activation Analysis. *Journal of Radioanalytical and Nuclear Chemistry*, 174 (2): 229-242.

Golitko, M., 2010. *Warfare and Alliance Building during the Belgian Early Neolithic, late sixth Millennium BC*. University of Illinois at Chicago, Ph. D. dissertation, 522p.

Golitko, M., 2011. Provenience investigations of ceramic and obsidian samples using laser ablation inductively coupled plasma mass spectrometry and portable X-ray fluorescence. *In* J.E. Terrell, E.M. Schechter (eds). *Exploring Prehistory on the Sepik Coast of Papua New Guinea*. Fieldiana Anthropology New Series No. 42. Field Museum of Natural History, Chicago, 251-287.

Golitko, M., 2015. *LBK Realpolitik: an archaeometric study of conflict and social structure in the Belgian early Neolithic*. Oxford, Archaeopress, 188p.

Golitko, M., Dussubieux, L., 2016. Inductively Coupled Plasma-Mass Spectrometry (ICP-MS) and Laser Ablation Inductively Coupled Plasma-Mass Spectrometry (LA-ICP-MS). *In* A.M.W. Hunt (ed.). *The Oxford Handbook of Archaeological Ceramic Analysis*. Oxford, Oxford University Press, 399-423.

Golitko, M., Sharratt, N., Williams, P.R., 2016. Open-Cell Ablation of Killke and Inka Pottery from the Cuzco Area: Museum Collections as Repositories of Provenience Information. *In* L. Dussubieux, M. Golitko, B. Gratuze (eds). *Recent Advances in Laser Ablation ICP-MS for Archaeology*. Natural Science in Archaeology, Berlin and Heidelberg, Springer Verlag, 27-52.

Gratuze, B., Blet-Lemarquand, M., Barrandon, J.-N., 2001. Mass spectrometry with laser sampling: A new tool to characterize archaeological materials. *Journal of Radioanalytical and Nuclear Chemistry*, 247 (30): 645-656.

Grave, P., Lisle, L., Maccheroni, M., 2005. Multivariate Comparison of ICP-OES and PIXE/PIGE Analysis of East Asian Storage Jars. *Journal of Archaeological Science,* 32: 885-896.

Guillaume, A., Meganck, M., 2004-2012. *Atlas du sous-sol archéologique de la Région de Bruxelles.* Direction des Monuments et des Sites, Musées royaux d'Art et d'Histoire, Bruxelles, vol. 13 à 24.

Guillaume, A., Meganck, M., 2007. *Atlas du sous-sol archéologique de la Région de Bruxelles.* Direction des Monuments et des Sites, Musées royaux d'Art et d'Histoire, Bruxelles, 17: 128-129.

Gurcke, K., 1987. *Bricks and brickmaking: A handbook for historical archaeology*. University of Idaho Press, 326 p.

Halkin, L.-E, Aubert, R., van Caenegem, R., Despy, G., Wyffels, C., 1970. *Monasticon belge, Province de Brabant*. Published by Centre national de recherches d'histoire religieuse, Liège, vol. 4.

Henne, A., Wauters, A., 1845. *Histoire de la Ville de Bruxelles*. Bruxelles, vol. 3.

Hollestelle, J., 1961. *De steenbakkerij in de Nederlanden tot omstreeks 1560*. Coll. Van Gorcum's Historische Bibliotheek, Assen, 66, 336 p., 77-82.

Hus, J., 2003. The magnetic fabric of some loess/palaeosol deposits. *Physics and Chemistry of the Earth*, 28: 689-699.

Hus, J., Ech-Chakrouni, S., Jordanova, D., 2002. Origin of magnetic fabric in bricks: its implications in archaeomagnetism. *Physics and Chemistry of the Earth*, 27: 1319–1331.

Hus, J., Ech-Chakrouni, S., Jordanova, D., Geeraerts, R., 2003. Archaeomagnetic investigation of two mediaeval brick constructions in North Belgium and the magnetic anisotropy of bricks. *Geoarchaeology*, 18 (2): 225–253.

Ingham, J.P., 2011. Petrography of geomaterial: a review. *Quarterly Journal of Engineering Geology and Hydrogeology*, The Geological Society of London, 44: 457–467.

Jochum, K.P., Weis, U., Stoll, B., Kuzmin, D., Yang, Q., Raczek, I., Jacob, D.E., Stracke, A., Birbaum, K., Frick, D.A., Günther, D., Enzweiller, J., 2011. Determination of Reference Values for NIST SRM 610–617 Glasses Following ISO Guidelines. *Geostandards and Geoanalytical Research*, 35 (4), December 2011: 397-429.

Kristály, F., Kelemen, É., Rózsa, P., Nyilas, I., Papp, I., 2011. Mineralogical investigations of medieval bricks samples from Béké County (SE Hungary). *Archaeometry*, 54 (2): 250-266.

Kuleff, I., Djingova, R., 1998. Mean concentration of elements determined in Ohio Red Clay. *Journal of Radioanalytical and Nuclear Chemistry,* 237 (1-2): 3-6.

Laenen, B., 1997. The geochemical signature of relative sea-level cycles recognised in the Boom Clay. Ph.D. thesis, K.U.Leuven, Leuven, Belgium.

Laleman, M.C., Stoops, G., 2008. Baksteengebruik in Vlaamse steden : Gent in de middeleeuwen. *In* T. Coomans, H. van Royen (eds). *Medieval Brick Architecture in Flanders and Northern Europe: the question of the Cistercian origin.* Abdijmuseum "Ten Duinen 1138", Koksijde & Academia Press publishers, , in ibid., 163-183.

Lanos, P., 1987. The effects of demagnetizing fields on thermoremanent magnetization acquired by parallel-sided baked clay blocks. *Geophysical Journal International, The Royal Astronomical Society,* 91: 985-1012.

Lanos, P., Kovacheva, M., Chauvin, A., 1999. Archaeomagnetism, methodology and applications: Implementation and practice of the archaeomagnetic method in France and Bulgaria. *European Journal of Archaeology*, 2: 365–392.

Lehouck, A., 2008. Gebruik en productie van baksteen in de regio Veurne van circa 1200 tot circa 1550. *In* T. Coomans, H. van Royen (eds). *Medieval Brick Architecture in Flanders and Northern Europe: the question of the Cistercian origin.* Abdijmuseum "Ten Duinen 1138", Koksijde & Academia Press publishers, , in ibid., 203-232.

Lindsey, D.A., 1999. An evaluation of alternative chemical classifications of sandstones. U.S. Department of the Interior, U. S. Geological Survey, Open-file report 99-346, 26p. From https://pubs.usgs.gov/of/1999/0346/report.pdf, consulted 02/2018.

López-Arce, P., Garcia-Guinea, J., Gracia, M., Obis, J., 2003. Bricks in historical buildings of Toledo City: characterisation and restoration. *Materials Characterization*, 50 (1): 59-68.

Maher, B.A., Thompson, R., 1995. Paleorainfall reconstructions from pedogenic magnetic susceptibility variations in the Chinese loess and paleosols. *Quaternary research*, 44: 383-391.

Martiny, V.-G., 1992. *Bruxelles: architecture civile et militaire avant 1900*. Published by J.M. Collet, Braine-l'Alleud.

Massart, C., 2001. Étude archéologique de l'impasse du Papier (1996). *In* P. Blanquart, S.Demeter, A. De Poorter, C. Massart, S. Modrie, I. Nachtergael, M. Siebrand (eds). *Autour de la première enceinte*. Collection : *Archéologie à Bruxelles*, 4: 262-326.

Meloni, S., Oddone, M., Genova, N., Cairo, A., 1999. The Production of Ceramic Materials in Roman Pavia: An Archaeometric NAA Investigation of Clay Sources and Archaeological Artefacts. *Journal of Radioanalytical and Nuclear Chemistry,* 224(3): 553-558.

Mertens, J., Vandenberghe, N., Wouters, L., Sintubin, M., 2003. The origin and development of joints in the Boom Clay Formation (Rupelian) in Belgium. *Geological Society London Special Publications,* 216 (1): 309-321.

Nunes, K.P., Toyota, R.G., Oliveira, P.M.S., Neves, E.G., Soares, E.A.A., Munita, C.S., 2013. Preliminary compositional evidence of provenance of ceramics from Hatahara archaeological site, Central Amazonia. *Journal of Chemistry*, 2013, 6p.

Pavía, S., 2006. The determination of brick provenance and technology using analytical techniques from the physical sciences. *Archaeometry*, 48 (2): 201-218.

Pavía, S., Roundtree, S., 2005. An investigation into Irish historical ceramics: the bricks of Arch Hall, Wilkinstown, CO, Meath. *Proceedings of the Royal Irish Academy*, 105C (6): 221-242.

Pettijohn, F.J., Potter, P.E., Siever, R., 1972. *Sand and Sandstone*. Springer-Verlag, Berlin, Heidelberg, New York, 618p.

Sapin, C., Baylé, M., Büttner, S., Guibert, P., Blain, S., Lanos, P., Chauvin, A., Dufresne, P., Oberlin, C., 2008. Archéologie du bâti et archéométrie au Mont-Saint-Michel, nouvelles approches de Notre-Dame-sous-Terre. *Archéologie médiévale*, 38 : 71-122.

Sosnowska, P., 2013. De briques et de bois. Contribution à l'histoire de l'architecture à Bruxelles. Étude archéologique, technique et historique des matériaux de construction utilisés dans le bâti bruxellois (13e-18e siècle) (3 vols). Ph.D thesis, Université libre de Bruxelles.

Sosnowska, P., 2014. Approach on brick and its use in Brussels from the 14th to the 18th century. *In* T. Ratilainen, R. Bernotas, C. Herrmann (eds). *Fresh Approaches to the Brick Production and Use in the Middle Ages*. Proceedings of the session (and more) "Utilization of Brick in the medieval period – Production, Construction, Destruction", Held in the European Association of Archaeologists (EAA) Meeting 29.8-1.9.2012 in Helsinki, Finland, British Archaeological Report, International series, 27-36.

Sosnowska, P., Goemaere, E., 2016. The reconstruction of Brussels after the bombardment of 1695: an analysis of the recovery through a historical and archaeological study of the use of bricks. *Construction History*, 31 (2): 59-80.

Sosson, J.-P., 2000. La brique aux Pays-Bas aux XIVe et XVe siècles : Production, prix, rentabilité. *In* P. Boucheron, H. Broise, Y. Thébert (eds.). *La brique antique et médiévale. Production et commercialisation d'un matériau*. Coll. De l'Ecole française de Rome, 247: 261-268.

Speakman, R.J., Neff, H., 2005. *Laser ablation ICP-MS in Archaeological Research*. University of New Mexico Press, Albuquerque, 201p.

Vandenberghe, N., De Craen, M., Wouters, L., 2014. The boom clay geology from sedimentation to present-day occurrence. A review. *Memoirs of the Geological Survey of Belgium*, 60: 78p.

Viaene, W., Ottenburgs, R., De Breuck, W., Gullentops, F., Vandenberghe, N., Bogemans, F., Mostaert, F., 1996. Keramische Delfstoffen. *Delfstoffen in Vlaanderen*, s.l., 29-52.

Waucquez, L., 2013. Le palais de Charles de Lorraine à Bruxelles. Un chantier dans la ville au XVIIIe siècle. Mémoire de master en histoire, Bruxelles, Université libre de Bruxelles.

Wets, T., 2008. Vroeg baksteengebruik in Brugge. *In* T. Coomans, H. van Royen (eds). *Medieval Brick Architecture in Flanders and Northern Europe: the question of the Cistercian origin.* Abdijmuseum "Ten Duinen 1138", Koksijde & Academia Press publishers, 147-162.

Wijffels, T., Nijland, T.G., 2004. Deterioration of historic brick masonry due to combined gypsum, ettringite and thaumasite: A case study. 13th international brick/block masonry conference, Amsterdam, 809-815.

Wolf, S., 2002. Estimation of the Production Parameters of Very Large Medieval Bricks from St. Urban, Switzerland. *Archaeometry*, 44 (1): 37-65.